MINISTÉRIO DA CIÊNCIA, TECNOLOGIA E INOVAÇÃO
INSTITUTO NACIONAL DE PESQUISAS ESPACIAIS

sid.inpe.br/mtc m21d/2023/02.08.13.42-TDI

THE CO2 FLUXES AND THEIR RELATIONSHIP TO ENVIRONMENTAL CONDITIONS ON THE SOUTHWEST ATLANTIC OCEAN AND ITS SOUTHERN OCEAN SECTOR

Celina Cândida Ferreira Rodrigues

Doctorate Thesis of the Graduate Course in Remote Sensing, guided by Drs. Luciano Ponzi Pezzi, and Marcelo Freitas Santini, approved in December 19, 2022.

URL of the original document:
<http://urlib.net/8JMKD3MGP3W34T/48GESAL>

INPE
São José dos Campos
2022

PUBLISHED BY:

Instituto Nacional de Pesquisas Espaciais - INPE
Coordenação de Ensino, Pesquisa e Extensão (COEPE)
Divisão de Biblioteca (DIBIB)
CEP 12.227-010
São José dos Campos - SP - Brasil
Tel.:(012) 3208-6923/7348
E-mail: pubtc@inpe.br

MINISTÉRIO DA CIÊNCIA, TECNOLOGIA E INOVAÇÃO
INSTITUTO NACIONAL DE PESQUISAS ESPACIAIS

sid.inpe.br/mtc m21d/2023/02.08.13.42-TDI

THE CO2 FLUXES AND THEIR RELATIONSHIP TO ENVIRONMENTAL CONDITIONS ON THE SOUTHWEST ATLANTIC OCEAN AND ITS SOUTHERN OCEAN SECTOR

Celina Cândida Ferreira Rodrigues

Doctorate Thesis of the Graduate Course in Remote Sensing, guided by Drs. Luciano Ponzi Pezzi, and Marcelo Freitas Santini, approved in December 19, 2022.

URL of the original document:
<http://urlib.net/8JMKD3MGP3W34T/48GESAL>

INPE
São José dos Campos
2022

Cataloging in Publication Data

Rodrigues, Celina Cândida Ferreira.

R618c The CO2 fluxes and their relationship to environmental conditions on the Southwest Atlantic Ocean and its southern ocean sector / Celina Cândida Ferreira Rodrigues. – São José dos Campos : INPE, 2022.

xxiv + 77 p. ; (sid.inpe.br/mtc m21d/2023/02.08.13.42-TDI)

Thesis (Doctorate in Remote Sensing) – Instituto Nacional de Pesquisas Espaciais, São José dos Campos, 2022.

Guiding : Drs. Luciano Ponzi Pezzi, and Marcelo Freitas Santini.

1. CO2 flux. 2. bulk methodology. 3. eddy covariance. 4. Southwest Atlantic Ocean. 5. Southern Ocean. I.Title.

CDU 528.8:551.5

MINISTÉRIO DA CIÊNCIA, TECNOLOGIA E INOVAÇÕES

INSTITUTO NACIONAL DE PESQUISAS ESPACIAIS
Serviço de Pós-Graduação - SEPGR

DEFESA FINAL DE TESE DE CELINA CÂNDIDA FERREIRA RODRIGUES
REG. 142949/2018, BANCA Nº 339/2022

No dia 19 de dezembro de 2022, por videoconferência, o(a) aluno(a) mencionado(a) acima defendeu seu trabalho final (apresentação oral seguida de arguição) perante uma Banca Examinadora, cujos membros estão listados abaixo. O(A) aluno(a) foi APROVADO(A) pela Banca Examinadora, por unanimidade, em cumprimento ao requisito exigido para obtenção do Título de Doutora em Sensoriamento Remoto. O trabalho precisa da incorporação das correções sugeridas pela Banca Examinadora e revisão final pelo(s) orientador(es).

Novo Título: "THE CO2 FLUXES AND THEIR RELATIONSHIP TO ENVIRONMENTAL CONDITIONS ON THE SOUTHWEST ATLANTIC OCEAN AND ITS SOUTHERN OCEAN SECTOR"

Membros da banca:

Dr. Márcio de Morisson Valeriano – Presidente – INPE
Dr. Luciano Ponzi Pezzi – Orientador – INPE
Dr. Marcelo Freitas Santini – Orientador – INPE
Dra. Leticia Cotrim da Cunha – Membro Externo – UERJ
Dra. Nathalie Lefèvre – Membro Externo – Institut Pierre-Simon Laplace - IPSL

Declaração de aprovação de Nathalie Lefèvre anexa ao processo.

Documento assinado eletronicamente por **Marcelo freitas Santini (E)**, **Usuário Externo**, em 03/01/2023, às 11:17 (horário oficial de Brasília), com fundamento no § 3º do art. 4º do Decreto nº 10.543, de 13 de novembro de 2020.

Documento assinado eletronicamente por **Márcio de Morisson Valériano**, **Tecnologista**, em 04/01/2023, às 11:17 (horário oficial de Brasília), com fundamento no § 3º do art. 4º do Decreto nº 10.543, de 13 de novembro de 2020.

Documento assinado eletronicamente por **Luciano Ponzi Pezzi**, **Pesquisador**, em 04/01/2023, às 17:38 (horário oficial de Brasília), com fundamento no § 3º do art. 4º do Decreto nº 10.543, de 13 de novembro de 2020.

Documento assinado eletronicamente por **Leticia Cotrim da Cunha (E)**, **Usuário Externo**, em 11/01/2023, às 12:43 (horário oficial de Brasília), com fundamento no § 3º do art. 4º do Decreto nº 10.543, de 13 de novembro de 2020.

A autenticidade deste documento pode ser conferida no site https://sei.mcti.gov.br/verifica.html, informando o código verificador **10680558** e o código CRC **D369CE32**.

Referência: Processo nº 01340.010220/2022-77 SEI nº 10680558

“Existe muita coisa que não te disseram na escola!
Cota não é esmola!”.

“Agora que eu comecei a escrever.
Que eu nunca me cale!
O jogo só vale quando todas as partes puderem jogar!”

Bia Ferreira

A minha mãe!

Que me ensinou que a felicidade está na simplicidade!

AGRADECIMENTOS

Como sempre na minha vida, agradeço a Deus por me abençoar nessa caminhada.

Aos meu orientadores, Dr. Luciano P. Pezzi e Dr. Marcelo F. Santini, pela grande oportunidade e por depositar bastante confiança em mim.

Ao Dr. Nathaniel Brunsell, pela grande oportunidade e ensinamentos durante o intercâmbio.

À minha mãe, que nas ações e gestos, nunca deixou faltar amor, compreensão e incentivos.

Aos professores do Programa de Pós-Graduação em Sensoriamento Remoto (PGSER), que pelos seus ensinamentos e conhecimentos transmitidos, foram muito importantes em nossa formação acadêmica.

Aos meus amigos de curso, que colaboraram para um aproveitamento acadêmico no sentido de conhecimento e companheirismo.

A CAPES, pela bolsa concedida para realização do doutorado.

ABSTRACT

The oceans play an important role in mitigating climate change by acting as large carbon sinks, especially at middle and high latitude regions. The main objective of this work is to investigate the behavior of turbulent CO_2 fluxes at medium- and high-latitude under different atmospheric and oceanic conditions, during the trajectories of research ships to the Southwest Atlantic Ocean and its portion in the Southern Ocean. The CO_2 flux was calculated using the eddy covariance and bulk methodology. During the experiment the Brazil Current sink more CO_2 than Malvinas Current, owing to its proximity to the chlorophyll-rich and less saline waters of the La Plata River, and intense wind speeds increased the CO_2 flux between the ocean and atmosphere. The Brazil Malvinas Confluence also behaved as a CO_2 sink, and the modulation of CO_2 fluxes was due to the intense horizontal gradient of SST together with the moderate surface wind and turbulence. The MC sequestered less carbon than other regions because of the presence of a high-pressure system near the region, low atmospheric turbulence, and light surface winds that inhibited mass exchange between the ocean and atmosphere. The Bransfield Strait uptake 38.59% more CO_2 than the Drake Passage due to the cold and fresh waters, allied to the influence of glacial meltwater dilution. The Drake Passage, on average, behaved as a CO_2 sink, mainly due to physical characteristics. To minimize the uncertainty in bulk methodology for CO_2 flux, we found the best fit for the gas transfer coefficient was $K = 0.2325*u^2 – 0.4361*u + 1.764$ with R^2 of 0.97, and it showed an adequate representation of ocean-atmosphere fluxes for Southwest Atlantic Ocean. The bulk methodology the purpose gas transfer coefficient had good agreement with the *in situ* data (eddy covariance) for the ACEx and and Antarctic Operations 32, 33, 34, and 37 (2012 to 2018). The Southwest Atlantic Ocean had been increasing the assimilation of carbon along the years analyzed (2003 to 2020), mainly due to the increase of CO_2 concentration in the atmosphere. This research contributes to a better understanding of the Southwest Atlantic Ocean and Southern Ocean's role in the global carbon balance.

Keywords: CO_2 flux. *Bulk* methodology. Eddy covariance. Southwest Atlantic Ocean. Southern Ocean.

OS FLUXOS DE CO_2 E SUA RELAÇÃO COM AS CONDIÇÕES AMBIENTAIS NO OCEANO ATLÂNTICO SUDOESTE E SEU SETOR NO OCEANO AUSTRAL

RESUMO

Os oceanos desempenham um papel importante na mitigação das mudanças climáticas, atuando como grandes sumidouros de carbono, especialmente nas regiões de latitudes médias e altas. O principal objetivo deste trabalho é investigar o comportamento dos fluxos turbulentos de CO_2 em latitudes médias e altas sob diferentes condições atmosféricas e oceânicas, durante as trajetórias de navios de pesquisa para o Oceano Atlântico Sudoeste e sua porção no Oceano Austral. O fluxo de CO_2 foi calculado usando a covariância de vórtices turbulentos e a metodologia bulk. Durante o experimento, a Corrente do Brasil sequestrou mais CO_2 do que a Corrente das Malvinas, devido à sua proximidade com as águas ricas em clorofila e menos salinas do Rio da Prata, e ventos intensos aumentaram o fluxo de CO_2 entre o oceano e a atmosfera. A Confluência Brasil Malvinas também se comportou como um sumidouro de CO_2, devido ao intenso gradiente horizontal de temperatura da superfície do mar, junto com ventos moderados e turbulência. A corrente das Malvinas sequestrou menos carbono do que outras regiões devido à presença de um sistema de alta pressão próximo à região, baixa turbulência e ventos fracos na superfície que inibiram a troca de massa entre o oceano e a atmosfera. O Estreito de Bransfield absorveu 38,59% mais CO_2 do que a Passagem de Drake devido às águas frias e menos salinas, aliadas à influência do degelo glacial. A Passagem de Drake, em média, comportou-se como um sumidouro de CO_2, principalmente devido às características físicas. Para minimizar as incertezas na metodologia bulk para o cálculo do fluxo de CO_2, encontramos o melhor ajuste para o coeficiente de transferência de gás foi K = 0,2325*u2– 0,4361*u+ 1,764 com R2 de 0,97, esse mostrou uma representação adequada dos fluxos para o Atlântico Sudoeste. A metodologia de bulk, aplicando o coeficiente de transferência de gás proposto, teve boa concordância com os dados *in situ* (covariância de vórtices turbulentos) para o ACEx e para as Operações Antárticas 32, 33, 34 e 37 (2012 a 2018). O Oceano Atlântico Sudoeste vem aumentando a assimilação de carbono ao longo dos anos analisados (2003 a 2020), principalmente devido ao aumento da concentração de CO_2 na atmosfera. Esta pesquisa contribui para uma melhor compreensão do papel do Oceano Atlântico Sudoeste e do Oceano Austral no balanço global de carbono.

Palavras-chave: fluxo de CO_2. Metodologia bulk. Covariância de vortíces turbulentos. Oceano Atlântico Sudoeste. Oceano Austral.

LIST OF FIGURES

Page

LIST OF TABLES

Page

LIST OF ABBREVIATIONS

ACEX	Atlantic Carbon Experiment
ALK	Alkalinity
ATMOS	Antarctic Modeling and Observation System
BC	Brazil Current
BM	Brazilian Marine
BMC	Brazil-Malvinas Confluence
BS	Bransfield Strait
chl	chlorophyll
Cint	Studies Center of Ocean-Atmosphere-Cryosphere Interaction
DP	Drake Passage
EC	Eddy Covariance
ENSO	El Niño-Southern Oscillation
H41	Almirante Maximiano
IPCC	Intergovernmental Panel on Climate Change
IRGA	Infrared Gas Analyzer
MABL	Marine atmospheric boundary layer
MAX	Maximum
MC	Malvinas Current
MIN	Minimum

MUR	Multi-scale Ultra-high Resolution
NOAA	National Oceanic and Atmospheric Administration
PF	Polar Front
Po/V	Navy Polar Vessel
PROANTAR	Brazilian Antarctic Program
SACCF	South Antarctic circumpolar front
SAF	Subantarctic front
SAM	Southern Annular Mode
SAO	Southwest Atlantic Ocean
SLP	Sea Level Pressure
SO	Southern Ocean
SSS	Sea Surface Salinity
SST	Sea Surface Temperature
TSM-Tar	Sea Surface Temperature - air temperature
WS	Weddell Sea
XBT	Expendable Bathythermograph

LIST OF SYMBOLS

CO_2	Carbon dioxide
FCO_2	CO_2 Flux
ρa	dry air density
w	vertical wind component
c	ratio of CO_2 to dry air density
$\vec{V}_{real}$	real wind speed vector at the moment of measurement
$\vec{V}_{obs}$	speed measured by the anemometer
$\vec{V}_t$	angular velocities
$\vec{w}$	angular velocities
$\vec{V}_n$	ship's travel speed
$\vec{r}$	anemometer position vector in relation to the motion sensor
T_{ae}	coordinate transformation matrix from the anemometer reference system to the earth coordinate system (x-axis, y-axis and z-axis)
u*	friction velocity
$k1$	Von Kármán
U_{10}	wind speed at 10 m above the surface
Δp_{CO_2}	difference of the p_{CO_2}between air and sea
s	CO_2 solubility in seawater
k	gas transfer velocity

$pCO_{2(eq)}$	partial pressure of CO_2 in the equilibrator
$xCO_{2(eq)}$	molar fraction of CO_2 in the equilibrator
P_{eq}	atmospheric pressure at equilibrator
P_{weq}	partial water vapor pressure at the equilibrator
$pCO_{2(sw)}$	CO_2 partial pressure in the ocean
T_{EQ}	temperature in the equilibrator
$pCO_{2(air)}$	partial pressure in the atmosphere
$xCO_{2(air)}$	molar fraction of CO_2
P_{atm}	atmospheric pressure
P_b	water vapor pressure at the temperature and salinity for mixed layer water
$f_{CO_{2\,(sw)}}$	CO_2 fugacity
u	wind speed
Sc	Schmidt number

CONTENTS

Page

1 INTRODUCTION

The greenhouse gas carbon dioxide (CO_2) has been increasing over 40% since industrial revolution due to anthropogenic activities. According to the ”Keeling curve” measured at Hawaii island, the annual mean atmospheric CO_2 concentration increases from 278 ppm in 1958 to 415 ppm in 2022. The CO_2 accumulation in the air is considered as one of the important environmental factors to boost global warming (IPCC, 2021; TAKAHASHI et al., 2002; SABINE et al., 2004; LE QUÉRÉ et al., 2014, 2015). The global average surface temperature in July 2022 was 1.15°C above the average for the comparison period of 1880-1920 (NOAA, 2022).

In the last decades, oceans have absorbed over a quarter of the anthropogenic CO_2 emitted to the atmosphere (LE QUÉRÉ et al., 2018; GRUBER et al., 2019). The oceans are responsible for sequestering approximately 1/3 of anthropogenic carbon emissions per year (CANADELL et al., 2007). The medium- and high-latitude oceanic regions are considered important regions for CO_2 sinks (LE QUÉRÉ et al., 2018, TAKAHASHI et al., 2009). The Atlantic Ocean is the most important CO_2 sink, providing about 60% of the global ocean uptake of the global anthropogenic CO_2 uptake from the atmosphere from 1870 to 1995 (TAKAHASHI et al., 2009; FRÖLICHER et al., 2015; LE QUÉRÉ et al., 2016, 2018). The South hemisphere, between 14° S to 50° S, is considered the major sink area, sink an average -1.05 Pg C y-1. Therefore, understanding the carbon exchange behavior in these regions is very important in the study of global carbon fluxes.

Relevant scientific questions about global climate involve the understanding of the interaction between the ocean and atmosphere (SANTINI et al., 2020; SOUZA et al., 2021; PEZZI et al., 2021). The CO_2 flux between ocean and atmosphere is complex because it needs knowledge of ocean physics, atmospheric physics, cloud physics, and chemistry, as well as biogeochemical cycles in general (ITO et al., 2018; MONTEIRO, et al., 2020; JIANG et al., 2014). The estimation of ocean CO_2 uptake is still biased by the uncertainty of parameterization of gas transfer velocity and ocean CO_2 fugacity. Moreover, the

in-situ data has limitation in terms of spatial and temporal covers. Therefore, the utilization of satellite data has been complement the *in situ* data, which help to improve our knowledge of CO_2 flux between ocean and atmosphere (BENALLAL et al., 2017; WANNIKHOFF et al., 2017; LOHRENZ et al., 2018).

The Southwest Atlantic Ocean plays a role in the weather and climate of south and southwest Brazil and other South American countries (PEZZI et al., 2015). The Southern Ocean provides major contributions to maintaining our planet's climate and plays an important role in the nutrient distribution to other oceans basins (FAY et al., 2018). Furthermore, in the scenario of climate change, studies that increase knowledge of how CO_2 turbulent flux behaves in Southwest Atlantic Ocean and in Southern Ocean is very important for assessing the global carbon budget.

2 OBJECTIVES

2.1 General objective

The main objective of this work is to investigate the behavior of turbulent CO_2 fluxes at medium- and high-latitude under different atmospheric and oceanic conditions, during the trajectories of research ships to the Southwest Atlantic Ocean and its portion in the Southern Ocean.

2.2 Specific objectives

a) Determine how the intense horizontal sea surface temperature gradient modulate CO_2 fluxes at Southwest Atlantic;
b) Investigate the behavior of CO_2 fluxes at the Drake Passage and the Bransfield Strait on high spatiotemporal resolutions;
c) Determine how the atmospheric stability condition modulates CO_2 flux between ocean and atmosphere in the Southwest Atlantic Ocean and its portion in the Southern Ocean;
d) Purpose an algorithm for Ocean CO_2 fugacity, and a gas transfer coefficient for the Southwest Atlantic Ocean, based on *in situ* data collected at that region;
e) Validate the CO_2 fugacity algorithm and gas transfer coefficient for other fields campaigns. By comparing the CO_2 fluxes obtained with bulk parameterization and the fluxes obtained by eddy covariance;
f) Analyze the temporal variability of CO_2 flux in the Southwest Atlantic Ocean and investigate how different oceanic and atmospheric variables impacts CO_2 flux;

This document structure is based on independent but complementing chapters, each chapter is a manuscript published or (to be) submitted to a scientific journal. The specific objectives will be met by the following chapters: a and c, Chapter 5; b and c by Chapter 4; d to f by Chapter 6.

3 DATA AND METHODOLOGY

3.1 Study area

The study areas include the Southwest Atlantic Ocean (SAO) (Figure 3.1), and the Atlantic sector of the Southern Ocean (SO), comprising Drake Passage (DP) and Bransfield Strait (BS), as seen in Figure 3.2.

Figura 3.1 – Route of the Brazilian Navy Polar Vessel (Po/V) Almirante Maximiano (H41) at Southwest Atlantic Ocean. Composite between 14 to 27 October 2018, Sea surface temperature (°C) - Multi-scale Ultra-high Resolution (MUR).

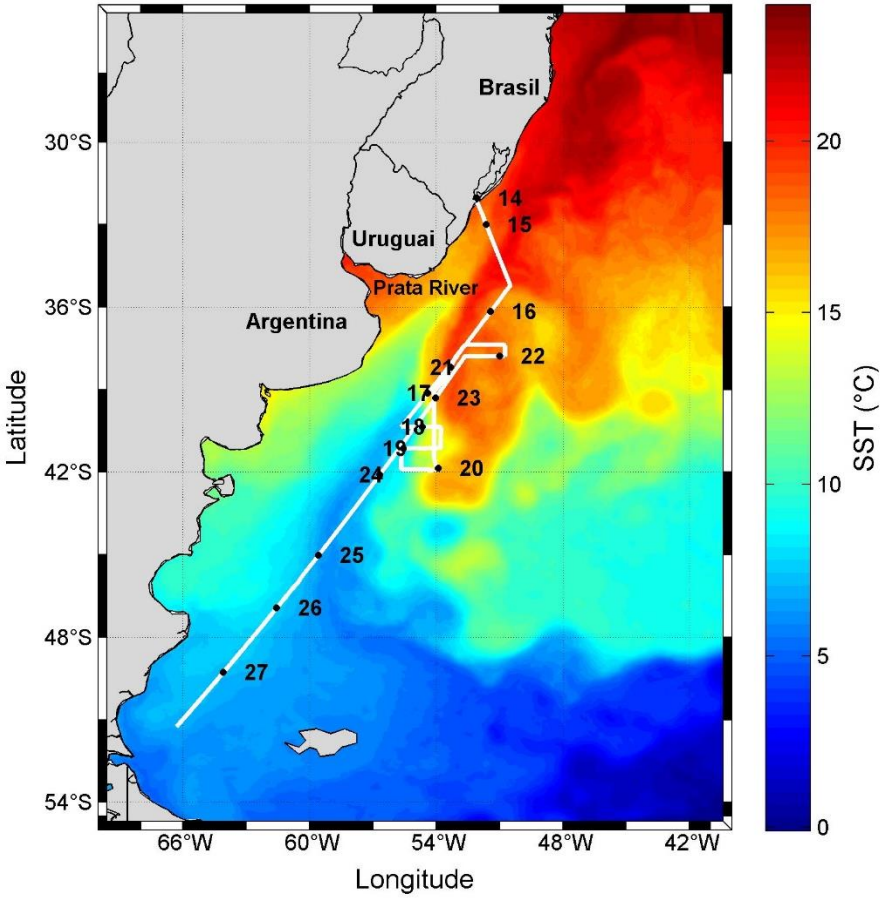

\

Source: Author's production.

Figura 3.2 – Route of the Brazilian Navy Polar Vessel (Po/V) Almirante Maximiano (H41) in the Southern Ocean. Composite between November 08 to 22 November 2018, Sea surface temperature (°C) derived from Multi-scale Ultra-high Resolution (MUR).

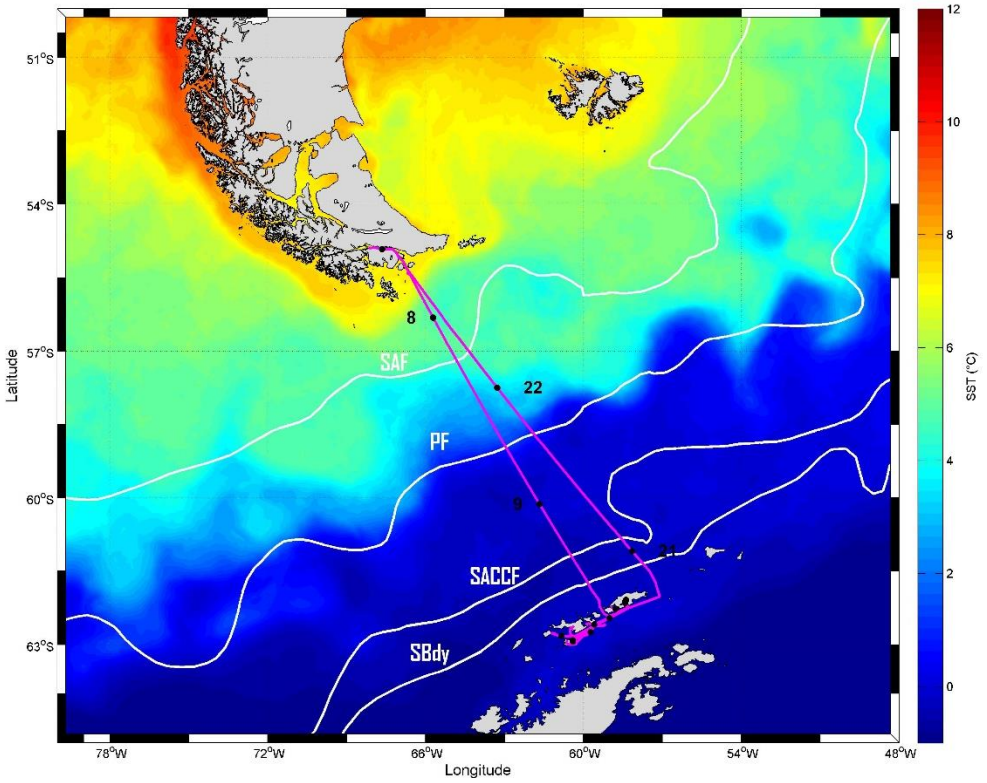

White lines: Subantarctic front (SAF), polar front (PF), South Antarctic circumpolar front (SACCF), and southern boundary (SBdy) are frontal positions as defined by Orsi et al. (1995).

Source: Author's production.

The Southwest Atlantic Ocean has great relevance for ocean-atmosphere interaction studies, especially because of its atmospheric characteristics. These include the frequent passage of atmospheric systems, such as cold fronts, cold air incursions, and cyclones, which present seasonal variability (REBOITA et al., 2010; HOSKINS; HODGES, 2005; PEZZI et al., 2009; GRAMCIANINOV et al., 2019). The climate of this area is characterized by strong seasonality owing to the South Atlantic subtropical high. This semi-permanent system is located at

approximately 30° S and 25° W. In summer, the system is less intense; it is located further south and east, but in winter, its center shifts north and west (CAMPOS, et al., 2014).

An intense horizontal SST gradient was characterized in the Southwest Atlantic Ocean. In this region, a front called the Brazil-Malvinas Confluence (BMC) is considered one of the most dynamic oceanic regions on the planet (CHELTON et al., 1990; CAVALCANTI et al., 2009). It is formed by the encounter between the warm waters of the Brazil Current (BC) and cold waters of the Malvinas Current (MC).

The main oceanic structure in the SO is the Antarctic Circumpolar Current. It is characterized by strong flows eastward that connect all ocean basins and is responsible for distributing physical and biogeochemical properties around the world (ORSI et al., 1995; RINTOUL et al., 2001; ITO et al., 2018). The SO is characterized by extreme winds, strong meridional temperature gradients, and high seasonal climate variability (e.g. sea ice cover; Swart et al., 2019).

The study region analyzed here is the Atlantic sector of the SO, comprising DP and BS at the east coastal region of the South Shetland Islands. They are in the northwest region of the Antarctic Peninsula and are influenced by waters coming from the southeast sector of DP, BS and the Weddell Sea (WS). The DP comprises the Subantartic front (SAF), Polar Front (PF), South Antarctic circumpolar front (SACCF), and southern boundary (SBdy, Figure 3.2). The region that goes from the Antarctic continent to the PF is the Antarctic Zone, and the region between the PF and the Subtropical Front is the Subantarctic Zone (ORSI et al., 1995).

The BS encompasses a transition zone between the Bellingshausen Sea and the WS. According to Lopez et al. 1999 this strait is mainly controlled by the interaction of two different fluxes: (i) the warmer and less saline waters from the Bellingshausen Sea (which enters on passages further west at South Shetland Islands) and (ii) the colder and more saline waters from the WS (which enters near the Joinville island). The frontal structure results from the meeting of these two currents, named the Bransfield Front. The BS also is influenced by Antarctic

Circumpolar Current that promotes intrusions of Circumpolar Deep Water associated to climatic modes (BARLLET et al., 2018). The DP waters also enter at BS, but stay near to the South Shetland Islands, and their interference at BS is negligible (ZHOU et al., 2002).

3.2 Data

In this thesis, a combination of *in situ* data, satellite data, and reanalysis data were used in the study area. Meteorological and oceanic data were collected on scientific cruises (Table 3.1), which were conducted in the Southwest Atlantic Ocean and its portion of the Southern Ocean, by using research ships from the Brazilian Marine (BM). These oceanographic cruises are part of the activities planned and developed by the Studies Center of Ocean-Atmosphere-Cryosphere Interaction (CInt) and for the Antarctic Modeling and Observation System (ATMOS) Project. Those projects surged in response to a Brazilian Antarctic Program (PROANTAR) scientific call.

Table 3.1 - Description of the cruises used in this thesis.

Oceanographic Cruise	Period	Study region	Research Ship
ACEX	2012	Southwest Atlantic Ocean	Cruzeiro do Sul
OP32	2013	Southwest Atlantic Ocean	NPo Alm. Maximiano
OP33	2014	Southwest Atlantic Ocean	NPo Alm. Maximiano
OP34	2015	Southwest Atlantic Ocean	NPo Alm. Maximiano
OP37	2018	Southwest Atlantic Ocean and Southern Ocean	NPo Alm. Maximiano

Source: Author's production.

The data of the Southwest Atlantic Ocean and Southern Ocean from OP37 is presented in Chapters 5 and 4, respectively. The data of the Southwest Atlantic

Ocean from ACEX, OP32, OP33, OP34, and OP37 were used in Chapter 6. The ship tracks are illustrated in Figure 3.1 and 3.2 are overlaid on the sea surface temperature (SST) field, which highlights the intense along track SST gradients, characteristic of the BMC presence and the Antarctic Circumpolar Current (ORSI et al., 1995); those tracks are part of the Chapters 4 and 5. The ship tracks used in Chapter 6 are illustrated in Figure 3.3.

Figure 3.3 - Routes of the Brazilian Navy research Vessel (RV) Cruzeiro do Sul (blue line; H38) and the Brazilian Navy Polar Vessel (Po/V) Almirante Maximiano (H41) and study area.

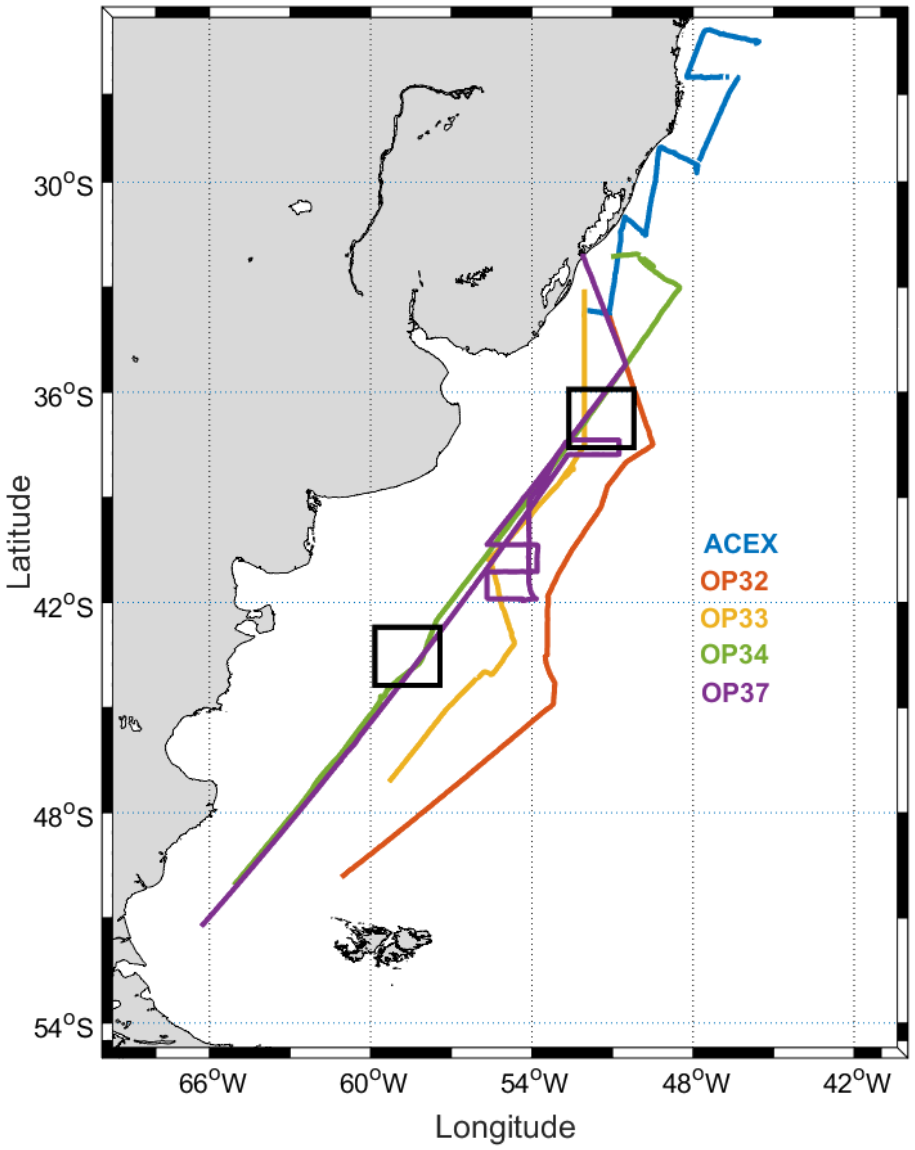

The ship routes are for the ACEX cruise (2012), OP 32, OP 33, OP 34, and OP 37 cruises (2012, 2013, 2014, 2015, and 2018, respectively). The black rectangle indicates the location of the data for variability climate of CO_2.

Source: Author's production.

3.2.1 Observed data

The data collected are divided into oceanic and meteorological data. The oceanic data are obtained through the thermosalinograph, a sensor attached to

the hull of the ships, which collects temperature and salinity values in the ocean surface layer. Also includes vertical seawater temperature data collected by XBT (Expendable Bathythermograph) probes.

Meteorological data are collected by the ship's Automatic Meteorological Station and by sensors installed in a micrometeorological tower (collected at high and low frequencies) at the bow of the ships. Also, it is used radiosondes, which are carried by weather balloons, and provide measurements of the thermodynamic (pressure, air temperature, and relative humidity) and dynamic (wind speed and direction) states of the atmosphere.

During the OP37, eight expendable bathy-thermographs were deployed at the locations where eight radiosondes were launched. This was because we aimed primarily to use ocean–atmosphere measurements made on the BMC to investigate its potential to locally change the atmosphere immediately above it. Those data are presented in Chapter 5.

3.2.1.1 Flux tower

The data sets used here were collected by a micrometeorological tower installed on the bow of the Brazilian Navy Polar Vessel (Po/V) Almirante Maximiano (H41) and Cruzeiro do Sul during the Atlantic Carbon Experiment (ACEX) project and Antarctic Operations 32, 33, 34, and 37 which occurred between 2012 and 2018.

The H41 and micrometeorological tower used in the campaign are shown in Figure 3.4. The micrometeorological tower was installed approximately 16 m above sea level with a similar setup used in previous cruises in the Southwestern Atlantic (PEZZI et al., 2016; OLIVEIRA et al., 2019; SANTINI et al., 2020; SOUZA et al., 2021). More recently this same setup was used in an oceanic mesoscale eddy turbulent flux study at Brazil-Malvinas Confluence (BMC) by Pezzi et al. (2021).

Figure 3.4 - Brazilian Navy Polar Vessel (Po/V) Almirante Maximiano (H41) with its micrometeorological tower during the OP37, between 14 to 27 October, and 08 to 22 November.

Source: Author's production.

For direct CO_2 turbulent fluxes measurements in the ocean-atmosphere interface, were used micrometeorological sensors sampling in high- and low-frequency rate (20 Hz and 0.06 Hz; Table 3.2). The sonic anemometer was fixed in a 1 m long metal bar installed perpendicularly to the vertical mechanical structure of the micrometeorological towers and forward to the ship's bows. This configuration allowed measurements to avoid the flow distortions of the ships' structure on the vertical component of the wind vector (SANTINI et al., 2020).

Table 3.2 - Description of the sensors installed in the micrometeorological tower, during the OP37, between 08 to 22 November 2018.

Data Source (sampling frequency)	**Sensor / Manufacturer**	**Meteorological Variable**
Micrometeorological Tower (20 Hz)	3D Sonic Anemometer and Gas Analyzer (IRGASON/CAMPBELL)	CO_2 concentration (mg m^3); H_20 concentration (g m^{-3}); u, v e w (m/s);
	Motion Pack II/ Systron Donner	Angular velocity (deg s^{-2}); Acceleration (m s^{-2})
	GPS/Garmin	Ship heading (°) Ship velocity (m/s)
Micrometeorological Tower (0.06 Hz)	PT101/CAMPBELL	Atmospheric pressure (hPa)
	HC2S3/VAISALA	Air temperature (°C); Relative humidity (%)

Source: Author's production.

The tower sensors were tested and calibrated by the Meteorological Instrumentation Laboratory of INPE before and after the experiment. The Infrared Gas Analyzer (IRGA) is calibrated following the manual instructions (CAMPBELL SCIENTIFIC, 2016) using two different gas concentrations of CO_2, and zero humidity concentration and dew point temperature for the H_2O. The first part of the procedure simply measures the CO_2 and H_2O zero and span, without making adjustments. This allows the CO_2 and H_2O gain factors to be calculated. These gain factors quantify the state of the analyzer before the zero-and-span procedure and were used to correct recent measurements for drift. The last part of the zero-and-span procedure adjusts internal processing parameters to correct subsequent measurements. For zero we used the Analytical Nitrogen 5.0 with minimum purity of the 99.999% to CO_2 and H_20. The CO_2 SPAN was obtained using N2 balanced CO_2 at a concentration of

396.45 +/- 0.05ppm. The H_2O SPAN was obtained using a Li-Cor LI-610, with the accuracy of ± 0.2 °C dew point.

3.2.2 Satellite and reanalysis data

The satellite and reanalysis data set were used as auxiliary data to complement the understanding of the surface characteristics of the ocean's mesoscale and synoptic atmospheric conditions in the study region. More details are presented in Table 3.3.

Table 3.3 - Satellite and reanalysis data used in this project.

Variable	Data Source	Spatial resolution	Temporal resolution
Chlorophyll	VIIRS Aqua MODIS	4 km	Daily Monthly
Salinity	SMOS ORAS5	0.25°	Daily Monthly
Sea Surface Temperature	ERA5 MUR	0.25° 1 km	Hourly and Monthly Daily
Wind speed and direction	ERA 5	0.25°	Hourly and Monthly
Sea Level Pressure	ERA 5	0.25°	Hourly and Monthly
Air Temperature	ERA 5	0.25°	Hourly and Monthly
xCO_2 atm	OCO_2 CAMS	2x2.5 km 0.25°	16 days Monthly

Source: Author's production.

3.3 Methodology

3.3.1 Eddy covariance method

The most used method by the scientific community for calculating turbulent fluxes from *in situ* measurements is Eddy Covariance (EC). EC is based on the

covariance between vertical wind velocity and the concentration of gases in the atmosphere, which results in fluxes between the surface and the atmosphere (ARYA, 2001; STULL et al., 1988). The carbon dioxide flux (FCO_2) is mathematically defined by Equation 3.1.

$$FCO_2 = \overline{\rho a\, w'c'} \tag{3.1}$$

Where FCO_2 is the CO_2 flux in μmol m^{-2} s^{-1}, the bars correspond to the means and the apostrophes indicate the turbulent fluctuations around the mean; ρa is the dry air density (kg m^{-3}), w' is the vertical wind component (m s^{-1}), c' is the ratio of CO_2 to dry air density (μmol mol^{-1}).

The wind data need the corrections prior to fluxes estimation, due to ship movement. The spurious fluctuations caused by these movements can be removed, with the methodology applied by Miller et al. (2008) and Edson et al. (1998) originally based on Fujitani (1981). The actual wind speed collected on a mobile platform can be estimated from Equation 3.2.

$$\vec{V}_{real} = T_{ae}\vec{V}_{obs} + T_{ae}\left(\vec{V}_t + \vec{w}\ x\ \vec{r}\right) + \vec{V}_n \tag{3.2}$$

Where $\vec{V}_{real}$ is the real wind speed vector at the moment of measurement; $\vec{V}_{obs}$ is the speed measured by the anemometer; $\vec{V}_t$ and $\vec{w}$ are the angular and linear velocities of the measuring equipment itself, respectively; $\vec{V}_n$ is the ship's travel speed; $\vec{r}$ is the anemometer position vector in relation to the motion sensor and T_{ae} is the coordinate transformation matrix from the anemometer reference system to the earth coordinate system (x-axis, y-axis and z-axis).

The flux uncertainty from the motion correction procedure is less than 6% (DONG et al., 2021). The flux bias due to the instrument calibration (gas analyzer, anemometer and meteorological sensors required to calculate air density: air temperature, relative humidity and pressure) is up to 4 %. However, this bias can reach up to 7% due to imperfection calibration of each sensor.

After the wind data correction, the turbulent flux calculations will be performed from the EC, by using the EddyPro ® software developed by LI-COR

Environmental. The gas analyzer used is open path, and it suffers from environmental effects that cause changes in air density and compromise the measurements, so this needs some corrections. In this software will be corrected the environmental interference (humidity, air temperature and atmospheric pressure in CO_2 density) called Webb Correction (WPL), developed by Webb et al. (1982). In addition, in this software will be set to remove spurious values and will calculate the average flux for 30 min.

Similar calculations based on EC were used in SW Atlantic for heat fluxes (PEZZI et al., 2016; SANTINI et al., 2020), momentum fluxes (HACKEROTT et al., 2018) and CO_2 fluxes (OLIVEIRA et al., 2019; PEZZI et al., 2021). Recently Pezzi et al. (2021) showed these calculations for heat and CO_2 fluxes over a warm core eddy in the SW Atlantic. A complementary variable used in this study is friction velocity (u*) (Equation 3.3). This variable gives us information about how turbulent the environment is (ARYA, 2001).

$$u^* = k1\, U_{10} \left(ln \frac{10}{z_0} \right)^{-1} \tag{3.3}$$

Where u^* is the friction velocity; $k1$ is the Von Kármán constant; U_{10} is the wind speed at 10 m above the surface.

3.3.2 *Bulk* methodology

The *Bulk* method development was based on the Monin-Obukhov similarity theory, which considers the constant flux in the surface layer that comprises 5 to 10% closest to the surface (FOKEN, 2008). For determining the gas flux, the Bulk method depends on the assumption that the transfer is given by the difference in gas concentration at the air-sea interface (MCGUILLIS et al., 2001). In addition, the method considers the gas solubility coefficient described by Weiss (1974) and the gas transfer velocity. An overview of the steps in the Bulk methodology is presented in Figure 3.5. This method is presented in chapter 6.

The carbon flux between the ocean and the atmosphere is given by Equation 3.4. However, partial pressure is sometimes expressed as fugacity that takes

into account the non-ideal nature of CO_2 gas (WEISS, 1974; EMERSON; HEDGES, 2008; TAKAHASHI et al., 2009; LENCINA-ÁVILA et al., 2016).

The partial pressure difference, $p_{CO_2 mar}$ - $p_{CO_2 ar}$ or Δp_{CO_2}, can be transformed to fugacity difference, Δf_{CO_2}.

$$F_{CO_2} = s \,.\, k \,.\, (\Delta p_{CO_2})_{sw-air} \quad \Leftrightarrow \quad F_{CO_2} = s \,.\, k \,.\, (\Delta f_{CO_2})_{sw-air} \qquad (3.4)$$

Where F_{CO_2} is the CO_2 flux (g m^{-2} s^{-1}) at the air-sea interface, the vertical gradient (Δp_{CO_2}) is the difference of the p_{CO_2} between air and sea (g m^{-3}); s is the CO_2 solubility in seawater (g m^{-3} µatm^{-1}), k is the gas transfer velocity (m s^{-1}).

Figure 3.5 - Flowchart for CO_2 flux calculation by Bulk Methodology.

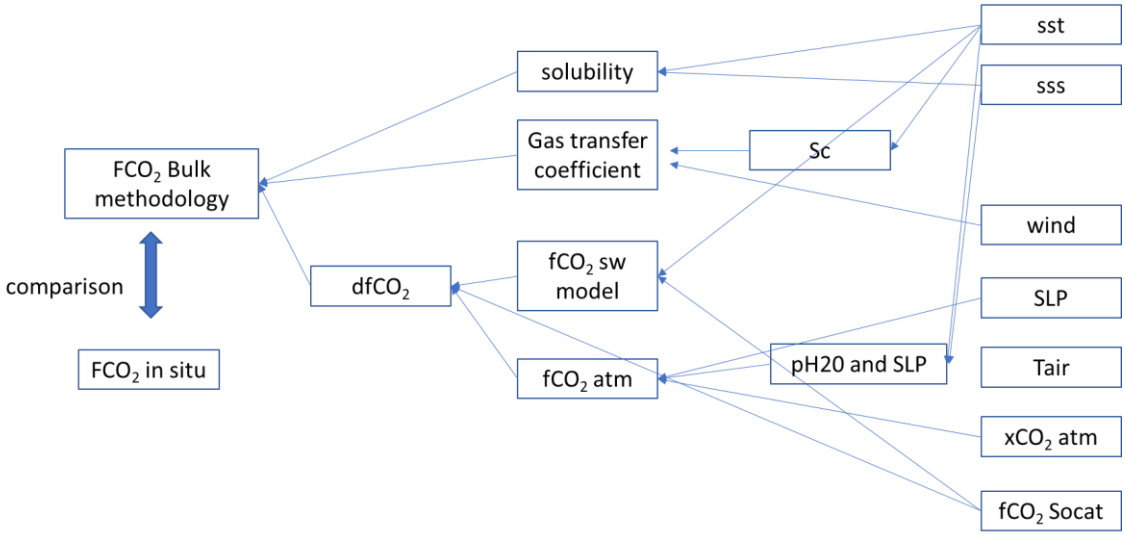

Source: Author's production.

3.3.2.1 Solubility

The CO_2 solubility in the ocean is calculated as a function of salinity (SSS) and SST (WEISS,1974):

$$ln\, s = A_1 + A_2(100/T) + A_3\, ln\,(T/100) + S[\,B_1 + B_2\,(T/100) + B_3\,(T/100)^2] \qquad (3.5)$$

where s is the solubility (mol kg^{-1} atm^{-1}); T is the SST (K) obtained by the MUR SST, and S is the salinity obtained by the SMOS. The values of the CO_2 specific constants (WEISS, 1974) A_1, A_2, A_3, B_1, B_2 and B_3, in mol L^{-1} atm^{-1}, can be found in Table 3.4.

Table 3.4 - Constants in mol kg^{-1} atm^{-1}.

Constant	Value
A1	-58.093
A2	90.5069
A3	22.294
B1	0.02777
B2	-0.0259
B3	0.00506

Source: Weiss (1974).

3.3.2.2 The CO_2 partial pressure at the air-sea interface

The difference in p_{CO_2} between the ocean and the atmosphere determines the direction of the flux. If $(\Delta p_{CO_2})_{mar-ar}$ is positive the flux will be from the ocean to the atmosphere, thus it indicates a carbon source region. If negative, the flux is from the atmosphere to the ocean, and the region would be considered a carbon sink (FARIAS et al., 2013; ITO et al., 2016).

The $p_{CO_2(sw)}$ data collected by Socat, is determined (BAKKER et al., 2013; 2014; PFEIL et al., 2013; SABINE et al.; 2013):

$$pCO_{2(eq)} = xCO_{2(eq)}\left(P_{eq} - P_{weq}\right) \qquad (3.6)$$

where $pCO_{2(eq)}$ is the partial pressure of CO_2 in the equilibrator; $xCO_{2(eq)}$ is the molar fraction of CO_2 in the equilibrator (ppm); P_{eq} is the atmospheric pressure at equilibrator (atm) and P_{weq} is the partial water vapor pressure at the equilibrator (atm).

The calculation of CO_2 concentration for seawater is defined according to Takahashi et al. (2009):

$$pCO_{2(sw)} = pCO_{2(eq)} exp\left[0.0423\left(SST - T_{eq}\right) - 4.35 * 10^{-5}\left(SST^2 - T_{eq}^2\right)\right] \quad (3.7)$$

where $pCO_{2(sw)}$ is the CO_2 partial pressure in the ocean; SST is the sea surface temperature (K); T_{eq} is the temperature in the equilibrator (K).

The $p_{CO_2(air)}$ is calculated as:

$$pCO_{2(air)} = xCO_{2(air)}(P_{atm} - P_w) \quad (3.8)$$

Where $pCO_{2(air)}$ is the CO_2 partial pressure in the atmosphere; $xCO_{2(air)}$ is the molar fraction of CO_2 (ppm); P_{atm} is the atmospheric pressure (atm) and P_w is the water vapor pressure at the temperature and salinity for mixed layer water (WEISS; PRICE, 1980).

3.3.2.3 Algorithm for CO_2 fugacity at ocean

The in-situ data of $f_{CO_2\,(sw)}$ from SOCAT were used to develop an algorithm, based on linear regression with SST from the ERA5, SSS from the SMOS and chl data from VIIRS. This algorithm for the determination of the $f_{CO_2\,(sw)}$ has the purpose of increasing temporal and spatial resolutions of the data for a better comparison with the ship data.

3.3.2.4 Gas transfer velocity

The main differences in carbon balance estimation are due to gas transfer velocity parameterization. Therefore, several methods of gas transfer velocity between the ocean and the atmosphere were assessed (Table 3.5).

Table 3.5 - Commonly used gas transfer (K) models assessed. Where u is the wind speed in m s^{-1} and Sc is the Schmidt number.

Reference	**Equation**
Wanninkhof (1992)	$if\ u \leq 6\ then\ K = 0.31\,u^2\left(\frac{Sc}{600}\right)^{-0.5}$ $else\ K = 0.39\,u^2\left(\frac{Sc}{600}\right)^{-0.5}$
Wanninkhof and McGillis (1999)	$K = 0.0283\,u^3\left(\frac{Sc}{600}\right)^{-0.5}$
Nightingale et al. (2000)	$K = (0.222\,u^2 + 0.333\,u)\left(\frac{Sc}{600}\right)^{-0.5}$
Jean-Baptiste, Fourré, and Poisson (2002)	$K = 1.45\,u^{1.5}\left(\frac{Sc}{310}\right)^{-0.5}$
Ho et al. (2006)	$K = 0.266\,u^2\left(\frac{Sc}{600}\right)^{-0.5}$
Sweeney et al. (2007)	$K = 0.27\,u^2\left(\frac{Sc}{600}\right)^{-0.5}$
Wanninkhof et al. (2009)	$K = 3 + 0.1\,u + 0.064\,u^2 + 0.011\,u^3\left(\frac{Sc}{600}\right)^{-0.5}$
Ho et al. (2011) (Equation (a))	$K = 0.286\,u^2\left(\frac{Sc}{600}\right)^{-0.5}$
Ho et al. (2011) (Equation (b))	$K = 0.0298\,u^3\left(\frac{Sc}{600}\right)^{-0.5}$
Wanninkhof (2014)	$K = 0.251\,u^2\left(\frac{Sc}{600}\right)^{-0.5}$
Pezzi et al. (2021)	$K = 0.34\,u^2 - 0.32\,u + 0.94$

Source: Author's production.

To determine the best model for the study area, each one was tested with wind speed data from ERA5. Then the flux was calculated by the *bulk* method and compared with the EC method. As a result of this process, a gas transfer

coefficient was proposed for the study region, which was based on the in-situ measurements of carbon fluxes by EC and bulk parameterization.

4 OCEAN-ATMOSPHERE TURBULENT CO_2 FLUXES AT DRAKE PASSAGE AND BRANSFIELD STRAIT[1]

4.1 Introduction

The main cause of global warming, according to the Intergovernmental Panel on Climate Change (IPCC) (IPCC, 2021), is the increase of greenhouse gases (GHG) emissions in the atmosphere since the pre-industrial period. Carbon dioxide (CO_2), one of the most important GHG, has increased by over 40% since the pre-industrial period. These values increased from 278 ppm in 1750 to 411.97 ppm in 2019, and the average global air temperature increased 0.89 °C between the years 1880 and 2019 (NOAA, 2019).

Relevant scientific questions about global climate involve the understanding of the interaction between the ocean and atmosphere (PEZZI et al. 2009; 2016; HACKEROTT et al., 2018; SANTINI et al., 2020; SOUZA et al., 2021; PEZZI et al., 2021). According to Canadell et al. (2007), the oceans are responsible for sequestering approximately 1/3 of anthropogenic carbon emissions per year. The CO_2 partial pressure in the ocean (pCO_{2sw}) has great spatial and temporal variability, being middle and high latitude regions considered CO_2 sinks (TAKAHASHI et al., 2009). The high latitudes have an important role in CO_2 exchange between ocean-atmosphere, which in turn are controlled by physical, chemical, and biogeochemical processes (ITO et al., 2018; MONTEIRo et al., 2020; JIANG et al., 2014).

Recent studies show that the Southern Ocean (SO) plays a major role in the global CO_2 cycle, accounting for 43% (42 Pg C) of the global anthropogenic CO_2 uptake from the atmosphere from 1870 to 1995 (TAKAHASHI et al., 2009; FRÖLICHER et al., 2015; LE QUÉRÉ et al., 2016; 2018). The SO sinks more CO_2 during the spring-summer than the autumn-winter due mainly to the sea-

[1] This article chapter is already accepted in the Annals of the Brazilian Academy of Sciences

ice cover retreats and biologically driven (RODEN et al., 2016; ITO et al., 2018; OGUNDARE et al., 2021).

Several modelling and observational studies suggest a reduction in the efficiency of SO CO_2 uptake over the past few decades (LOVENDUSKI et al., 2013; 2015; LE QUÉRÉ et al., 2010; METZL, 2009). Nevertheless, other studies suggest that global ocean uptake of CO_2 has increased over the past decade, largely due to the SO (LANDSCHÜTZER et al., 2014; MAJKUT et al., 2014; MUNRO et al., 2015; XUE et al., 2015). There is a need for studies that allow a better understanding of the processes involved in the exchange between the ocean and the atmosphere, at different spatiotemporal scales. Understanding how CO_2 turbulent flux behaves in different oceanic regions is very important for global carbon budget studies. The Atlantic Carbon and Fluxes Experiment (ACEx) project (PEZZI et al., 2016), the Ocean-Atmosphere Interaction Program in the Brazil-Malvinas Confluence Region (INTERCONF) (PEZZI et al., 2005; 2009), Southern Ocean Studies for Understanding Global Climate Issues (SOS-CLIMATE; ORSELI et al., 2017; ITO et al., 2018; MONTEIRO et al., 2020), Programme de Coopération avec l'Argentine pour l'e´tude de l'océan Atlantique Austral (ARGAU CRUISES; BIANCHI, et al., 2009) and more recently the Antarctic Modeling Observation System (ATMOS) project (PEZZI et al., 2021), are some of the South America research programs dedicated to study the exchange of ocean-atmosphere turbulent fluxes in the Southwest Atlantic Ocean (SAO) and the SO.

The observations in the Drake Passage (DP) show higher pCO_{2sw} values located in the north of the Antarctic Polar Front (PF) than to the south (MUNRO et al., 2015). Additionally, the seasonal cycle amplitude north of the front is much larger and well defined than south of the front. In the south of the PF has been a persistent CO_2 sink, due to the pCO_{2sw} being lower than the CO_2 partial pressure in the atmosphere (pCO_{2atm}) (CAETANO et al., 2020), influenced by the cold sea surface temperature (SST) during the summer and the presence of the upwelling of waters with low anthropogenic CO_2 content (PARDO et al., 2014) and mixed layer depths greater in winter (STEPHENSON et al., 2012).

The upwelling of old and CO_2 rich waters around Antarctica influences the carbonate system in the NAP environments (LENCINA-AVILA et al., 2018, MONTEIRO et al., 2020). It increases the macronutrients and CO_2 and decrease the carbonate concentration; however, those changes vary depending on mixing processes in response to sea ice, eddies formation, topography, and atmospheric forces (HENLEY et al., 2019). At the Northern Antarctic Peninsula, the coastal waters of the straits and bays are considered the most productive areas in the SO (COSTA et al., 2020). However, according to Caetano et al. (2020), the Bransfield Strait (BS) in late spring indicates a near-neutral air-sea CO_2 flux with a slight source to the atmosphere. Those authors suggest the temperature-sensitive metabolic and physical-chemical process cause significant impact on the spatial distribution of pCO_{2sw} at the BS.

Due to the major role in understanding climate, the biogeochemical cycles, the global energy balance, mass and energy fluxes are important study fields (TRENBERTH, 2009; TAKAHASHI, et al. 2009; LE QUÉRÉ et al., 2018; FAY et al., 2018). Changes in energy and mass fluxes between the ocean and atmosphere are controlled mainly by wind speed, air and sea temperature, humidity, radiation and evaporation (SATO, 2005). The SO provides major contributions to maintaining our planet's climate and plays an important role in the nutrient distribution to other oceans basins (FAY et al., 2018). However, due to its distance and hostility and adverse nature, it is difficult to collect *in situ* data (PEZZI et al., 2021; MONTEIRO et al., 2020). *In situ* data is typically collected in the summer because the complex environment for experimentation. Therefore, the utilization of satellite data have been complement the *in situ* data, which help to improve our knowledge of the role of the SO in the global climate (SHUTLER et al., 2016; BENALLAL et al., 2017; WANNIKHOFF et al., 2017; LOHRENZ et al., 2018).

The main objective of this work is to investigate the behavior of CO_2 fluxes at the Drake Passage and the Bransfield Strait west coastal areas under different atmospheric and oceanic conditions, during the Spring of 2018 on high

spatiotemporal resolutions when compared with traditional CO_2 fluxes estimations.

4.2 Results and discussion

The study region was split into two areas during H41 cruise, the DP and the BS, due to the different oceanic and atmospheric characteristics found between them. The CO_2 fluxes varied along the ship's route. Table 4.1 summarizes all data for the study region (DP, BS and total area). The CO_2 fluxes data were discarded under atmospheric stable conditions when the Monion-Obukhov stability parameter was greater than 0.2 (here, $\zeta > 0.2$). This is due to the inaccuracy in measuring turbulent fluxes when the turbulence is very small or intermittent (SUN et al., 2018; YUSUP; LIU, 2016; PATTEY et al., 2002).

Table 4.1 - Mean, maximum and minimum of the atmospheric and oceanic variables during ship's route.

		CO_2 flux	SLP	Wind speed	u*	SST-Tar	SSS	SST	chl
Drake Passage	mean	-1.70	980.94	15.48	0.33	-0.24	34.00	1.45	0.27
	max	21.38	993.40	20.29	0.56	2.47	34.28	5.31	0.64
	min	-11.46	967.35	1.30	0.08	-1.99	33.64	-0.76	0.10
Bransfield Strait	mean	-2.77	972.04	7.17	0.37	-1.21	33.76	-0.13	0.26
	max	47.84	994.35	20.73	0.90	1.70	34.22	0.32	0.41
	min	-41.05	953.08	1.00	0.08	-5.92	33.40	-0.76	0.19
Total area	mean	-2.49	973.22	9.27	0.36	-0.97	33.80	0.26	0.26
	max	47.84	994.35	20.73	0.90	2.47	34.38	5.31	0.64
	min	-41.05	953.08	1.00	0.08	-5.92	33.40	-0.76	0.10

Mean, maximum, and minimum values of the Ocean-atmosphere CO_2 fluxes (CO_2 Flux) (mmol $m^{-2}d^{-1}$); Sea Level Pressure (SLP) (hPa) (Air Pressure), Wind speed (m s^{-1}); and Friction velocity (u*) (m s^{-1}), Sea Surface Salinity (SSS); Sea Surface Temperature (SST) (°C); Chlorophyll-a concentration (chl) (mg m^{-3}); for the Drake Passage, Bransfield Strait and Total area. Values obtained along the ship track and the data were collected in the OP37 during the period of 08 to 22 November 2018.
Source: Author's production.

Our experiment was conducted during the Spring of 2018 (08 to 22 November 2018), which may have impacted on fluxes direction, and as a result both areas, DP and BS, acted on average as CO_2 sink. Those results agree the mean behavior for those areas for the entire season (MUNRO et al., 2015; MONTEIRO et al., 2020). However, the variability of the pCO_{2sw}, may affect the flux results during the season. The pCO_{2sw} at DP changes during the spring, as seen by Fay et al. (2018), where their values were higher at the beginning of the season. Munro et al. (2015) found at DP, at the south of the PF, that the increasing pCO_{2sw} is slower than pCO_{2atm}, making this area a persistent CO_2 sink. The phytoplankton blooms typically occur at south of DP during spring

(CARRANZA; GILLE, 2015). At the BS for late spring, photosynthesis decreases the CO_2 partial pressure in the surface seawater, enhancing ocean CO_2 uptake (CAETANO et al., 2020).

The BS uptake on average 38.59% more CO_2 than DP, as shown in Table 4.1. This difference is attributed to the variability of both atmospheric and oceanic conditions along the H41's route. During the study period, the mean SST decreased from the DP towards BS (Figure 3.2 and Table 4.1). The SSS data did not cover the entire area, there was just some data especially for the BS region. The chl data also has gaps, due to clouds cover in this area during cruise period. These gaps are a result of how chl is obtained, which is through a passive sensor that suffers interference from the clouds on its quality measurements. The BS presented more turbulence in the atmosphere boundary layer, with a maximum u* value of 0.9, allied to that the wind speed reached maximum value, 20.7 m s^{-1}.

The BS is characterized by colder waters than DP, which increases the CO_2 solubility and due the difference of partial pressure of carbon dioxide (ΔpCO_2) between ocean and atmosphere, that may direct the fluxes to the ocean. In addition, during the sampled period, the BS had a predominance of stable atmospheric conditions contributing to the region act as a CO_2 sink. The stability condition is observed in the marine atmospheric boundary layer (MABL), it is due to the difference between SST - T_{air} (Figure 4.1). The SST-T_{air} at the near-surface interface is an atmospheric stability parameter that indicates the preferential surface flux direction. When SST - T_{air} > 0, MABL is unstable, and when SST - Tair < 0, MABL is stable (PEZZI et al. 2005; 2009; 2016; CAMARGO et al., 2013). Besides, during the ship's route, light to moderate rain occurred on some days. This rainfall allied to the influence of glacial meltwater dilution could reduce the salinity concentration in the ocean, also could induce the upwelling of nutrient-rich water supporting declines in pCO_{2sw} if light is not limiting for primary producers. The glacial meltwater inputs could influence in carbonate chemistry, by the dilution of carbonated ion concentration, so with a reduction of pCO_{2sw}. This condition, combined with colder waters that increase

the ocean CO_2 solubility, could favors the CO_2 fluxes to be directed to the ocean. This result suggests the complexity of the factors controlling the spatial distribution of pCO_{2sw} in BS. Similar results were found by Ito et al. 2018, for this region. The authors also investigated the role played by surface waters in controlling the pCO_{2sw} and sea-air CO_2 fluxes in the Northern Antarctic Peninsula region. For the BS, during the Summer of 2009, the physical effects such as glacial meltwater discharges, oceanic fronts and eddies, thermodynamic effects and stratification of the mixing layer also modified the pCO_{2sw} variability. When considering the BS, the biological processes were responsible for the CO_2 sink in this area, but during 2009, the physical processes dominated, and the area was a weak source of CO_2. Caetano et al. (2020) suggested the temperature might cause significant variability in the ocean surface distribution of CO_2 over short shoreline distances in the Northern Antarctic Peninsula. During the period from 14 to 15 November 2018, the ship was near to a low pressure atmospheric system as seen in Figure 4.2a e 4.2b and produced strong winds at the surface (~ 17 m s^{-1}) as well as high-friction velocities (~ 0.8 m s^{-1}; Figure 4.1). These factors favored the vertical mass movement and the ocean surface mixing that driving the fluxes to the ocean. According to Wanninkhof and Triñanes (2017), the increase in wind speed affects the absorption of CO_2 by the oceans regardless of the direction of flow.

Figure 4.1 - Time series of oceanographic and meteorological variables along the ship's track.

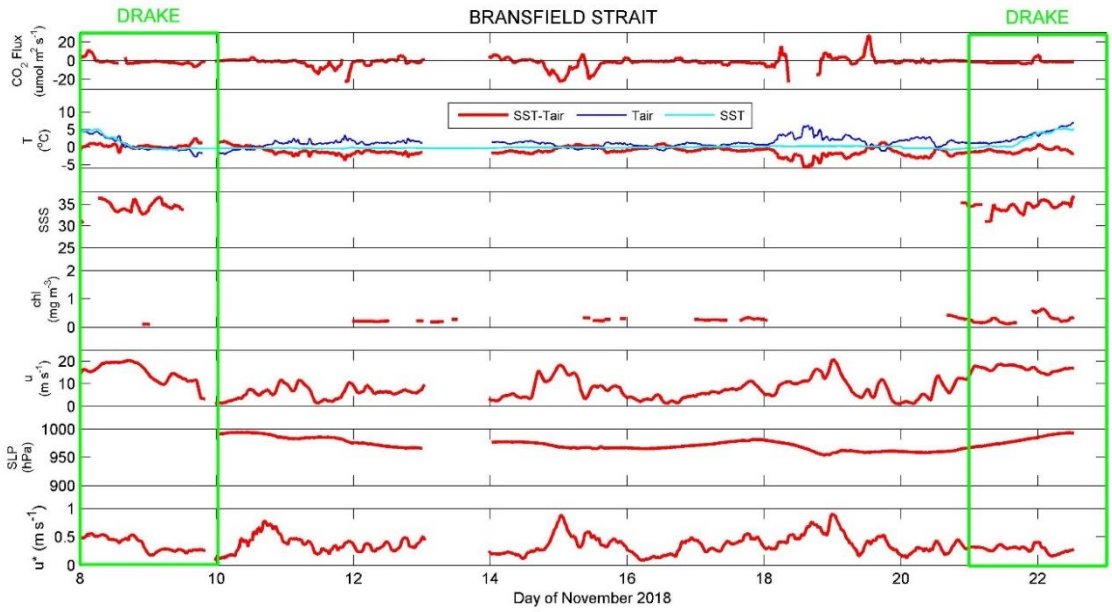

Time series of oceanographic and meteorological variables taken along the Po/V H41 route, from 08 to 22 November 2018. Ocean-atmosphere CO_2 fluxes (CO_2 Flux) (µmol m^{-2} s^{-1}); Sea Surface Temperature - air temperature (TSM-Tar) (°C), Sea Surface Temperature (SST), and Air temperature (Tair) (°C); Sea Surface Salinity (SSS); Chlorophyll-a concentration (chl) (mg m^{-3}); Wind speed (m s^{-1}); Sea Level Pressure (hPa) (SLP) and Friction velocity (u*) (m s^{-1}) The green rectangle separates the 2 areas: Drake Passage and Bransfield Strait.

Source: Author's production.

Figure 4.2 – Mean sea level pressure (blue lines), wind direction (arrows) and Po/V H41 location (black point) during the days 14, 15 e 19 November 2018, 00H for each day. Data from ERA5.

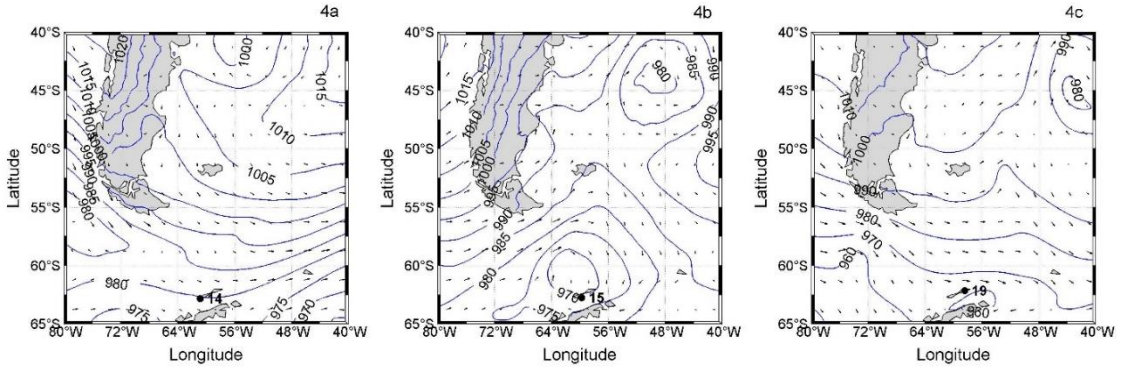

Source: Author's production.

However, changes in pCO_{2sw} under the influence of glacial meltwater input in the BS region, could influence the CO_2 flux behavior. The glacial meltwater and sea-ice melting input modify the surface layer stability and favors the development of phytoplankton blooms (VARELA et al., 2002). Changes in the salinity, derived from freshwater input, may cause the nitrate (NO3-) reduction caused by biological utilization reducing seawater alkalinity that has as consequence the increase of the pCO_{2sw} becoming sources of CO_2 (TAKAHASHI et al., 2014) as observed some peaks on days of November 15, 18 and 19. Monteiro et al. (2020) found the Northern Antarctic Peninsula absorbed more CO_2 in the Spring and Summer than Autumn and Winter. Those authors showed in the Northern Antarctic Peninsula, in autumn and winter, upwelling events that increased the remineralized carbon in the sea surface, leading the region to act as a CO_2 source to the atmosphere. Furthermore, the peak on 19 November 2018, where the ocean acted as a source of CO_2, was due to a combination of some other factors: proximity of a low atmospheric pressure system, with approximately 950 hPa (Figure 4.2c) and light to moderates surface winds (less than 10 m s^{-1}). Those factors contributed to the vertical movement in the MABL, thus decreasing CO_2 concentrations in the atmosphere near the ocean surface. As a result, the CO_2 fluxes were directed from ocean to atmosphere, with a mean value of 20 µmol m^{-2} s^{-1} (Figure 4.1).

On the other days 10, 12, 16, 17 and 20 of November 2018, the CO_2 fluxes were near the neutrality, with a stable MABL and low turbulence, thus inhibiting the mass exchange at the ocean-atmosphere interface

The DP on average behaved as a sink of CO_2 as seen in Table 4.1 and Figure 4.3a. The main causes were associated with the colder SST (1.45 °C), and fresher (34.44) waters as seen in Table 4.1. Thereby, the water properties such as SST and SSS had more impact on CO_2 fluxes compared to the presence of chl, which had low concentration at DP. The Figure 4.3a shows in the south of the PF has acted as a CO_2 sink, due to the pCO_{2sw} being lower than the pCO_{2atm} (MUNRO et al., 2015), influenced by the cold and fresh water. However, the CO_2 fluxes at DP are less intense than at BS, due to the presence of the intense upwelling process around 60 – 65 °S, which increases remineralized carbon to the surface (TAKAHASHI et al., 2012; HENLEY et al., 2020). The mean pCO_{2sw} for the DP was 368 µatm, value higher than as found by Fay et al. (2018), it was approximately 355 µatm in November of the period between 2002 and 2016, in DP. Similar results were found for Ito et al. 2018 in this region, for summer 2008. In their study which took place in the Northern Antarctic Peninsula and observed the role of surface water on controlling pCO_{2sw} and air CO_2 flux, the DP also presented a low concentration of chl. However, in this study in the summer of 2008, DP acted as a source of CO_2. The surface chl concentration is a proxy for the presence of primary production that has a role in the air-sea CO_2 fluxes as they may have a significant control on the gas partial pressure in the seawater (MONTEIRO et al., 2020; HENLEY et al., 2020). Song et al. (2015) discovered in their investigation the role of mesoscale eddies in modulating air-sea CO_2 flux in DP. In this study, the mesoscale eddies SST had a negative correlation with pCO_{2sw} in the ocean during the summer. Moreover, they highlighted that the dissolved inorganic carbon has more impact on CO_2 modulation than it does on temperature. However, Munro et al. (2015) reported the importance of the DP in the CO_2 sink for the SO during winter, especially in the south of the PF. Previous studies had reported the impacts of the SST and SSS on CO_2 fluxes, e.g., Wolf et al. (2016). And, found that SST has more considerable effects on the CO_2 ocean

solubility (WOLF et al., 2016). This can may the main cause that led to less CO_2 assimilation by the ocean, at DP, where the warmer waters in this region produced less solubility of CO_2 in the ocean when compared to the BS.

Figure 4.3 - a) Ocean-atmosphere CO2 fluxes (CO2 Flux) (µmol m−2 s−1), and b) pCO2sw (µatm) with Po/V H41 route at Drake Passage during the days 8, 9, 21 e 22 November 2018.

a)

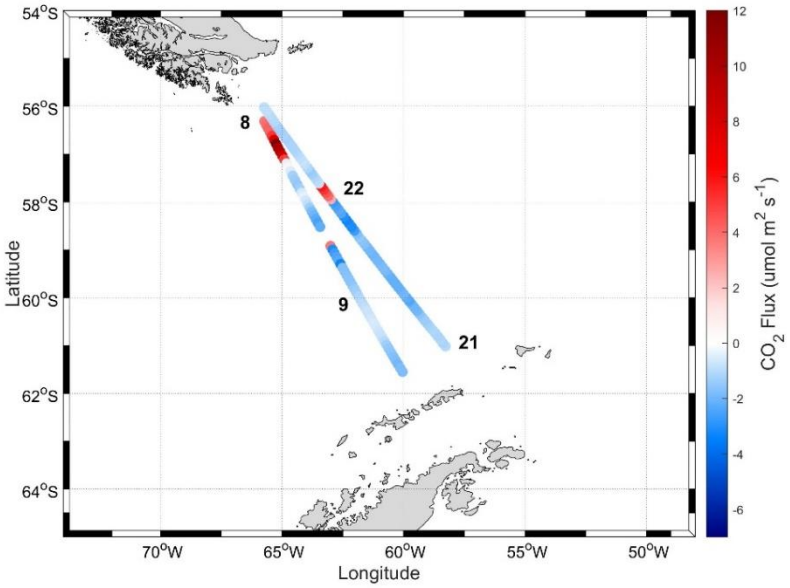

b)

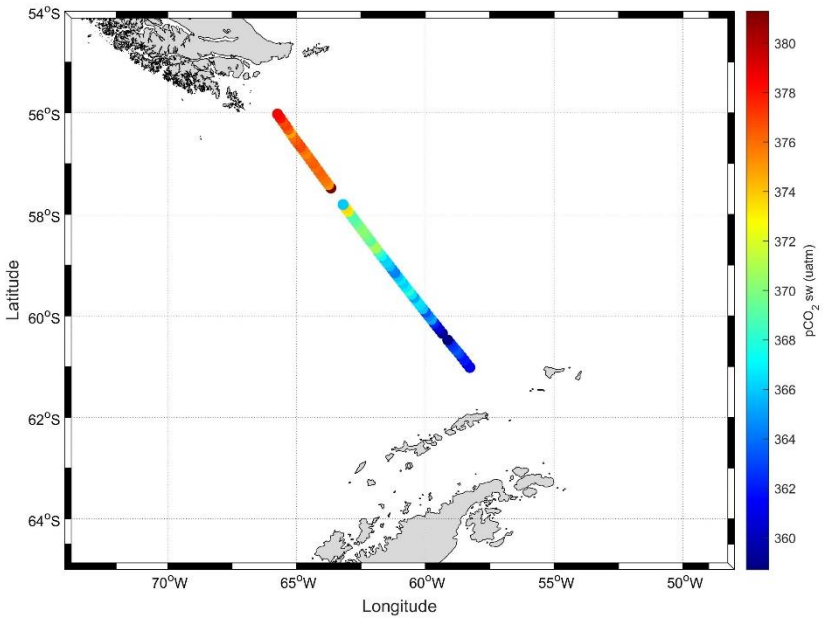

Source: Author's production.

At DP the ocean acted as a source of CO_2 to the atmosphere as seen in the CO_2 flux peaks during 8 and 22 of November 2018 (Figure 4.1 and 4.3a). Those days the ship was located at the north of the PF, that region has similar pCO_{2sw} and pCO_{2atm}, indicating near-neutral air-sea CO_2 flux or slight source to the atmosphere, those results are similar to the Munro et al. 2015 and Caetano et al. (2020). The pCO_{2sw} on the PF north was higher than to the south (Figure 4.3b), with mean values of 375 µatm, similar values found Ito et al. 2018. Moreover, this fact is also related to the unstable condition observed in the MABL observed during those days produced an intensification of the wind speed at surface and above it within MABL vertical extension. Consequently, more turbulence was produced and shown by the u*, which favored the transfer of mass between the sea surface and the atmosphere (WANNINKHOF; TRIÑANES, 2017). On the following days, 9 and 21 November 2018, when the ship was surveying over DP, the CO_2 fluxes were near to zero as seen in Figure 4.1 and 4.3a. In other words, there was no mass exchange between the ocean and the atmosphere. In this period, there was a predominance of low turbulence of less than 0.5 m s^{-1} (Figure 4.1), which inhibited the CO_2 fluxes.

The climate modes of variability, such as El Niño-Southern Oscillation (ENSO) and Southern Annular Mode (SAM), impact the variability of the surface carbonate system especially on interannual scale. During the November of 2018 the El Niño was active and SAM was in a positive phase, in this case, some studies indicate more CO_2 uptake in the Northern Antarctic Peninsula (BROWN et al., 2019, COSTA et al., 2020). However, other studies have opposites results, they found that in the positive SAM phase the ocean acted as a CO_2 source due to the reduction in biological activities (LOVENDUSKI et al., 2007; LEUNG et al., 2015). Another study did not find any effect of the SAM on the CO_2 carbon sink variability for 35 years (KEPPLER; LANDSCHÜTZER, 2019). Our study period (8 to 22 November 2018) was conducted during a positive and active phase of the SAM and El Niño, and the area was a sink of CO_2. The results could have some influence of those climate modes of variability. However, it is difficult to address the sink CO_2 behavior in the area due to the climate modes of variability. The influence of ENSO and SAM

changing the carbonate system parameters still not well understood in the scientific community.

4.3 Conclusions

This study showed the impacts of different atmospheric and oceanic conditions on the ocean-atmosphere CO_2 fluxes based on a combination of *in situ*, satellite, and reanalysis data sets. The *in situ* CO_2 fluxes data were collected in the DP and the BS in the second phase of OP37, covering the period from 8 to 22, November 2018. The CO_2 fluxes were obtained with the Eddy Covariance method (MILLER et al., 2008; PEZZI et al., 2021). The synoptic oceanic conditions were analyzed with chlorophyll, SSS and SST from satellites. The atmospheric synoptic conditions were obtained through ERA5 reanalysis data set analyzing T_{air}, SLP, wind speed and direction.

The BS and DP behaved as CO_2 sinks on average, where the main cause was attributed to the colder water that intensified the CO_2 solubility in the ocean. Comparing the mean value of CO_2 fluxes, the BS uptake on average 38.59% more CO_2 than DP. The DP, on average, behaved as a sink of CO_2 mainly due to physical characteristics. The south of the PF, DP has acted as a persistent CO_2 sink, due to the pCO_{2sw} being lower than the pCO_{2atm}, influenced by the cold and fresh water. However, the CO_2 fluxes at DP are less intense than at BS, due to the presence of the intense upwelling process around 60 – 65 °S, which increases remineralized carbon to the surface. There were some peaks of source of CO_2 in the north of the PF at DP, due to the unstable conditions of the atmosphere.

The BS was characterized by its colder waters compared to the DP, that contributes to the ocean act as sink. Furthermore, during the ship's route, light to moderate rainfall was recorded in some days. This rainfall may have contributed to the reduction of salinity concentration in the ocean, thus decreasing pCO_{2sw}, directing the fluxes toward the ocean, or minimizing the CO_2 outgassing. In addition, during the sampled period, the BS had a predominance of stable atmospheric conditions contributing to the region act as a CO_2 sink. However, during the period there were some peaks of CO_2 source

at BS, due to the reduction of seawater alkalinity by the glacial meltwater and sea-ice melting inputs, as consequence the increase of the pCO_{2sw}. Allied to that, the proximity of a low atmospheric pressure system and light to moderate turbulence and wind at the surface, thus it contributed to the vertical movement in the MABL.

This study supports the hypothesis that ocean-atmosphere CO_2 fluxes are highly dependent on oceanographic and meteorological conditions. This study also contributes to an improved understanding of the importance of the SO in the global carbon balance. The provided evidence shows that it is necessary to continue with observational campaigns in this region, to expand the knowledge about the SO's role in the global carbon dioxide cycle.

5 CO_2 FLUXES UNDER DIFFERENT OCEANIC AND ATMOSPHERIC CONDITIONS IN THE SOUTHWEST ATLANTIC OCEAN

5.1 Introduction

Atmospheric CO_2 concentrations, one of the most important greenhouse gases, has increased 40% since the beginning of the pre-industrial period (1750) and reached 416 ppm in 2021. This is considered a critical threshold for global climate change; the average global air temperature increased by 0.89 °C over the period 1880–2019 (NOAA, 2019). Therefore, there has been an increase in research focused on determining factors that may lead to intensification or reduction in CO_2 effects on the Earth's climate (LE QUÉRÉ et al., 2017).

Oceans are responsible for sequestering approximately 1/3 of anthropogenic carbon emissions annually (CANADELL et al., 2007), thereby attracting interest in the study of the CO_2 flux from the atmosphere to the ocean in response to the increasing CO_2 concentration in the atmosphere. Takahashi et al. (2009) showed that medium- and high-latitude oceanic regions are considered important regions for CO_2 sinks. The South Atlantic Ocean is the most important CO_2 sink, providing approximately 60% of the global ocean uptake, whereas the Southern Ocean contributes about 20% of the global carbon sink (TAKAHASHI et al., 1997). Bianchi et al. (2009) affirmed that the Southwest Atlantic Ocean represents one of the largest global carbon sinks. Using data obtained from 14 cruises between 2000 and 2008, Padin et al. (2010) demonstrated that the open ocean area behaved as a CO_2 source (sink) in spring (fall), whereas the continental shelf behaved as a CO_2 source in both seasons. Lencina-Avila et al. (2016) investigated the CO_2 flux and the sea-air CO_2 fugacity along the 35° S latitude between the South America and South Africa continent during the spring and summer of 2011. They found that owing to the physical variables of the South Atlantic Ocean, the entire area behaved as a CO_2 sink, with an average of -3.1 mmol m^{-2} d^{-1}. Moreover, Carvalho et al. (2021) identified that phytoplankton groups in the coastal South Atlantic Ocean are responsible for decreasing the partial pressure of CO_2 in the ocean (pCO_{2sw}) in the region. However, Ito et al. (2016) found that the coastal water in the Southwestern

Atlantic Ocean acted as a CO_2 source owing to the mesoscale physical processes during spring 2010 and summer 2011. Arruda et al. (2015) used a regional ocean biogeochemical model to investigate the processes responsible for the spatio-temporal variability in pCO_2 and the air-sea CO_2 fluxes in the southwestern Atlantic Ocean. They found that the continental shelf acted as a weak CO_2 source; south of 30° S, the region acted as a CO_2 sink, but to the north, there was an equilibrium between CO_2 of the ocean and the atmosphere. According to them, biological production and solubility are the main processes that regulate pCO_2 in the ocean. Pezzi et al. (2021) showed clear spatial correlations in CO_2 fluxes with the marine atmospheric boundary layer (MABL) stability over a warm core eddy surrounded by cold waters, which acted as a CO_2 source with an average of 0.3 mmol m^{-2} d^{-1}.

Many important scientific questions about the global climate involve understanding the interaction between the ocean and atmosphere (PEZZI et al., 2009; 2016; HACKEROTT et al., 2018; SANTINI et al., 2020). Therefore, understanding the carbon exchange behavior in these regions is very important in the study of global carbon fluxes. The Atlantic Carbon and Fluxes Experiment (ACEx) project (PEZZI et al., 2016), Ocean-Atmosphere Interaction Program in the Brazil-Malvinas Confluence Region (INTERCONF) (PEZZI et al., 2005; 2009), Southern Ocean Studies for Understanding Global Climate Issues (SOS-CLIMATE; ORSELI et al., 2017; ITO et al., 2018; MONTEIRO et al., 2020), Programme de Coopération avec l'Argentine pour l'étude de l'océan Atlantique Austral (ARGAU CRUISES; BIANCHI et al., 2009), and more recently the Antarctic Modeling Observation System (ATMOS) project (PEZZI et al., 2021), are some of the South American research programs dedicated to studying the exchange of ocean-atmosphere turbulent fluxes in the Southwest Atlantic Ocean and Southern Ocean.

Investigation of the behavior of the MABL in these interactions is of great scientific importance, because the exchange of properties in this layer between the atmosphere and ocean plays an important role in understanding climate variability, biogeochemical cycles, and the global energy balance

(TRENBERTH, 2009). Changes in energy and mass fluxes between the ocean and atmosphere are controlled mainly by wind speed, air and sea temperatures, humidity, radiation, and evaporation (SATO, 2005).

The Southwest Atlantic Ocean plays a role in the weather and climate of south and southwest Brazil and other South American countries (PEZZI et al., 2015). Thus, studies that increase knowledge of the ocean-atmosphere processes in this region are important for improving weather forecasts (PEZZI; SOUZA, 2009). Despite their importance, ocean-atmosphere fluxes are poorly sampled throughout the Southwest Atlantic Ocean compared with other regions, and there remains a critical need for systems designed to provide high-quality measurements in all seasons and sea states.

The main objective of this study was to investigate the behavior of turbulent CO_2 fluxes and quantify them over an intense horizontal sea surface temperature (SST) gradient in the Southwest Atlantic. This focus was provided by the opportunity for observing distinct synoptical atmospheric conditions during an oceanographic cruise aboard the Brazilian polar ship in the austral spring of 2018.

5.2 Results and discussion

The results and discussion is divided in the follow way: Section 3.1 brings the temporal series for CO_2 flux and other oceanic and atmospheric variables, during the trajectory of the ship between October 14 to 27, 2018. And the influence of those variables in CO_2 flux. The Section 3.2 presents a synoptic snapshot of the thermal structure of the MABL and ocean mixed layer produced at the BMC between October 16 and 17, 2018. And it's influence on the CO_2 flux.

5.2.1 Superficial analysis

The trajectory of Po/V H41 (Figure 3.1) started on October 14, 2018 in the warm waters of the Brazilian Coastal Current (BCC) and ended on October 27, 2018 in the cold waters of the MC. During this trajectory, the study region was split into four areas using satellite data from SST (Figure 3.1), SSS, and chl (Figure

5.1) because of the different oceanic and atmospheric conditions between them. The regions were the BCC, BC, BMC, and MC. Table 5.1 summarizes all data for the study region (BCC, BC, BMC, MC, and total area). The CO_2 flux varied along the path of the ship (Table 5.1 and Figure 5.3a). For detecting the differences between average CO_2 values between the regions, the Tukey's test was applied at 95% confidence level. Differences between the study areas were detected (Table 5.2). These differences are attributed to the variability in atmospheric and oceanic conditions along the path of the ship. The CO_2 flux data were discarded under stable atmospheric conditions when the Monin–Obukhov stability parameter was greater than 0.2 (here, $\zeta > 0.2$) as inaccuracies occur in measuring turbulent fluxes when turbulence is very small or intermittent (SUN et al., 2018; YUSUP; LIU, 2016; PATTEY et al., 2002).

Figure 5.1 - Composite for the period between 14 to 27 October 2018, Sea surface salinity data from Soil Moisture Active Passive (SMAP) (left); Chlorophyll (mg m^{-3}) data from VIIRS SNPP (right).

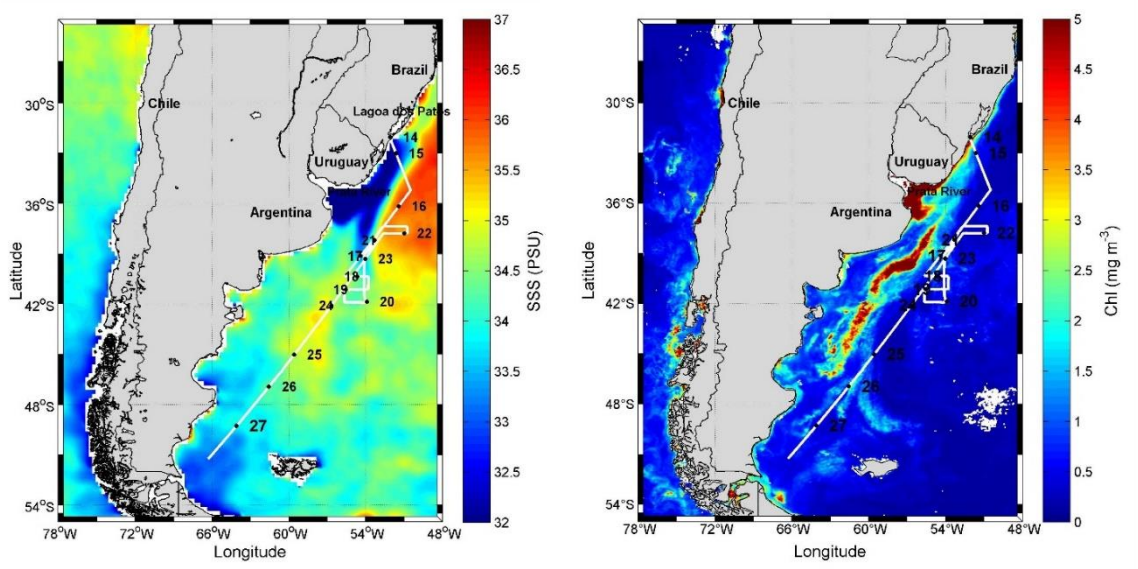

Source: Author's production.

Table 5.1 - Mean, maximum, and minimum values of the variables during ship's track.

		CO_2 Flux	SST	SSS	chl	Tair	u	u*	P
BCC	MEAN	-1.05	17.03	31.52	1.41	16.51	3.30	0.09	1014.05
	MAX	-0.19	17.52	32.27	2.56	16.89	4.73	0.22	1014.45
	MIN	-1.79	16.70	30.09	0.87	16.16	2.56	0.06	1013.45
	SUM	-18.91							
	STD	0.54	0.28	0.49	0.53	0.27	0.67	0.04	0.23
BC	MEAN	-2.90	19.29	35.55	0.38	16.84	11.66	0.36	1011.94
	MAX	0.30	22.26	36.31	1.95	19.71	20.80	0.69	1021.00
	MIN	-17.11	16.71	31.92	0.21	9.92	1.48	0.16	1005.78
	SUM	-529.97							
	STD	3.52	1.14	1.08	0.28	1.79	4.64	0.11	4.53
BMC	MEAN	-2.07	14.11	34.01	1.24	11.12	7.26	0.36	1018.39
	MAX	11.88	24.64	36.28	4.38	16.95	13.42	0.71	1027.43
	MIN	-13.58	6.95	31.98	0.05	6.83	1.24	0.11	1006.80
	SUM	-397.69							
	STD	3.80	5.44	0.79	0.96	2.31	3.05	0.13	7.12
MC	MEAN	-0.48	9.22	33.15	0.78	7.51	8.87	0.32	1017.24
	MAX	16.12	17.26	34.16	2.36	9.95	18.88	0.74	1025.47
	MIN	-19.43	6.41	31.72	0.13	5.99	2.92	0.10	997.29
	SUM	-111.63							
	STD	4.48	2.70	0.62	0.45	0.87	3.81	0.18	8.49
ALL	MEAN	-1.69	13.83	34.06	0.88	11.55	9.03	0.34	1015.97
	MAX	16.12	24.64	36.31	4.38	19.71	20.80	0.74	1027.43
	MIN	-19.43	6.41	30.09	0.05	5.99	1.24	0.06	997.29
	SUM	-1058.19							
	STD	4.07	5.39	1.35	0.73	4.23	4.29	0.15	7.46

Mean, maximum, and minimum values of the Ocean-atmosphere CO_2 fluxes (CO_2 Flux) (µmol m^{-2} s^{-1}); Sea Level Pressure (SLP) (hPa) (Air Pressure), Wind speed (m s^{-1}); Friction velocity (u*) (m s^{-1}), Sea Surface Temperature - air temperature (TSM-Tar) (°C); Sea Surface Salinity (SSS); Sea Surface Temperature (SST) (°C); Chlorophyll-a concentration (chl) (mg m^{-3}); for the Brazil Coastal Current (BCC), Brazil Current (BC), Brazil Malvinas Confluence (BMC), Malvinas Current (MC) and Total Area (All). Values obtained along the ship track and the data were collected in the OP37 during the period of 14 to 27 October 2018.

Source: Author's production.

Table 5.2 - Tuckey test with 95% confidence for average CO_2 fluxes (CO_2 Flux) (µmol m^{-2} s^{-1}) for Brazil Current, Brazil-Malvinas Confluence, Malvinas Current and Brazil Coastal Current in the OP37 during the period of 14 to 27 October 2018.

Areas	CO_2 Flux (µmol m^{-2} s^{-1})	Test results
Brazil Current	-2.90	a1
Brazil-Malvinas Confluence	-2.07	a1
Malvinas Current	-0.48	a2
Brazil Coastal Current	-1.05	a3

Source: Author's production.

The BCC was strongly influenced by discharge from the La Plata River; the mean value of chl concentration was 1.41 mg m^{-3} and the lowest SSS value was 27.70 (Table 5.1). These characteristics favored the behavior of this region as a CO_2 sink (Kerr et al., 2015), with an average of -1.05 µmol of CO_2 m^{-2} s^{-1} (Table 5.1). These biochemical processes (SSS and chl) have more impact on the flux direction than do the physical processes such as SST, with an average of 17.03 °C. The chl data had gaps owing to cloud cover in this area during the cruise period. These gaps are because chl is obtained through a passive sensor which is affected by interference from clouds and thereby influences the quality of measurements. Carvalho et al. (2021) recently identified phytoplankton groups that strengthen the CO_2 uptake in the BCC. A similar behavior was found by Orselli et al. (2019) in their study of the impact of Agulhas eddies on sea–air CO_2 fluxes in the South Atlantic Ocean. They found that the entire region along the Agulhas corridor in the South Atlantic Ocean acted as a CO_2 sink in July 2015 (austral winter). However, Ito et al. (2016) found that the South Atlantic Ocean on the Southern Brazilian Shelf acted as a CO_2 source during the late spring of 2010 and the early summer of 2011. According to them, both

regional upwelling and mesoscale physical processes, such as fronts, meanders, and eddies, have a major influence on the spatial distribution of the sea surface pCO_{2sw} over the region. Arruda et al. (2015) found that the southwestern South Atlantic Ocean on the inner continental shelf acts as a weak CO_2 source. In addition, the MABL was under neutral conditions on October 14 and 15, 2018, as can be seen by the SST-T_{air} difference (Figure 5.2), which inhibits intense exchange between the ocean and atmosphere. The stability parameter is based on the difference between the SST and T_{air}, and the surface layer is unstable when SST > T_{air} (PEZZI et al., 2005; 2009; 2016; CAMARGO et al., 2013).

Figure 5.2 - Time series of atmospheric and oceanographic variables along the ship's track.

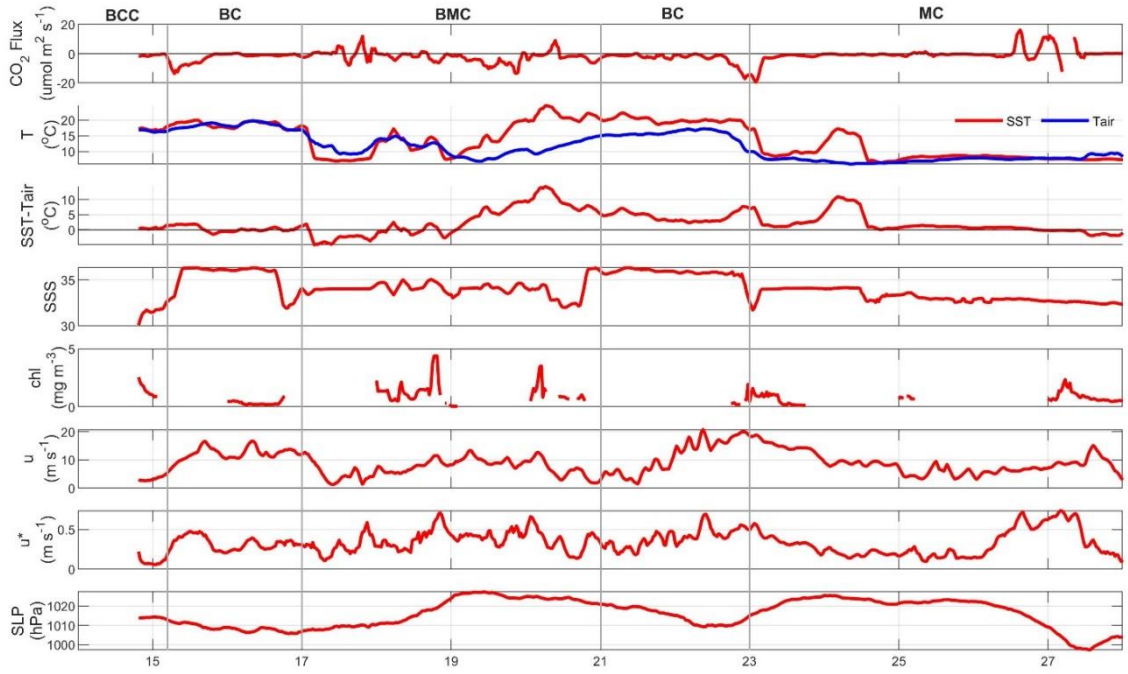

Time series of atmospheric and oceanographic variables taken along the Po/V H41 route, from 14 to 27 October of 2018. Ocean-atmosphere CO_2 fluxes (CO_2 Flux) (µmol m^{-2} s^{-1}); Sea Surface Temperature (SST) (°C); Air Temperature (T_{air}); Sea Surface Salinity (SSS); Chlorophyll-a concentration (chl) (mg m^{-3}); Wind speed (u) (m s^{-1}); and Friction Velocity (u*) (m s^{-1}); Sea Level Pressure (SLP) (hPa). The gray lines separate the four areas BCC, BC, BMC and MC.
Source: Author's production.

The characteristics of BC favor the ocean to behave as a source of CO_2, such as the highest mean SSS value (35.55), highest mean SST value (19.29 °C), and lowest chl concentration (0.38 mg m^{-3}) (Table 5.1). However, this area has higher uptake of CO_2 than the other regions, with an average of -2.90 µmol of CO_2 m^{-2} s^{-1} (Table 5.1). A similar pattern was found by Padin et al. (2010), who used data obtained from 14 cruises between 2000 and 2008 and showed that the open ocean in the southwestern South Atlantic Ocean behaved as a CO_2 sink in spring. The largest uptake of CO_2 by the ocean occurred on October 15 and 22, 2018 (Figure 5.2) owing to the proximity to the chl-rich and less saline waters of the La Plata River and the cold and less saline waters of the MC, respectively. On October 15, 2018, the meeting of less saline water from BCC with the more saline water from BC resulted in a density difference owing to which there was a subduction of BC, thus contributing to CO_2 assimilation on this day (Figures 3.1, 5.1, and 5.2). On October 22, 2018, there was a meeting between the BC and MC, and the presence of chl and low SST resulted in a CO_2 sink (Figures 3.1, 5.1, and 5.2). Furthermore, the intensification of wind speed (Figure 5.2) favors mass transfer to the ocean (Wanninkhof; Triñanes 2017) and such increases in wind speed affect the CO_2 exchange between the ocean and atmosphere, regardless of the direction of the fluxes. On the remaining days, October 16 and 21, 2018, the ship was in the BC and the CO_2 fluxes were practically null. This is because the high-pressure system acting on the study region (Figure 5.4a and 5.4b) with low turbulence ($u^* < 0.5$ m s^{-1}) inhibited vertical movements in this region.

The BMC was the second region that absorbed a large amount of CO_2, with an average of -2.07 µmol CO_2 m^{-2} s^{-1}; however, according to the Tukey test, there was no significant difference when compared with the BC (Table 5.2). Padin et al. (2010) found that the BMC area has the highest CO_2 uptake along the Atlantic Ocean owing to the variability in SSS, SST, and strong winds. The BMC is a region that presents an intense horizontal temperature gradient (PEZZI et al., 2016; HACKEROTT et al., 2018; SANTINI et al., 2020) formed by the meeting of the warm waters of the BC with the cold waters of the MC (Figures 3.1 and 4.5b). Thus, this region exhibits an intense oscillation in the CO_2 flux

(Figures 5.2 and 5.3a). On October 19, 2018, there was increased absorption of carbon by the ocean owing to the position of the ship in the cold and less saline water, in addition to the predominance of a moderate wind speed of 10 m s^{-1} and turbulence of approximately 0.5 m s^{-1} (Figures 5.1 and 5.2), which contributed to the mass exchange between the ocean and atmosphere. There were peaks in the CO_2 fluxes between October 17 and 18, 2018, when the ocean acted as a source of CO_2 to the atmosphere (Figures 5.2 and 5.3a). This is related to the presence of warm and saline water owing to the route of the ship being close to the BC waters (Figures 3.1, 5.1, and 5.2). Moreover, turbulence was moderate, with u* approximately 0.5 m s^{-1} (Figure 5.2), which contributed to the CO_2 exchange. There was also a peak during October 20, 2018, owing to the instability of the atmosphere, as SST > T_{air}, combined with turbulence greater than approximately 5 m s^{-1} and wind speed of approximately 10 m s^{-1}. In such a case of an unstable atmosphere, there is more turbulence and agitation of the particles, resulting in a decrease in the CO_2 concentration in the atmosphere close to the ocean. In addition, in this region, the presence of hot water (>20 °C) reduces CO_2 solubility and increases the pCO_2 in the oceans. This difference in pCO_2 between the ocean and atmosphere directs the fluxes to the atmosphere. Several studies have reported the effect of SST and salinity on CO_2 fluxes; however, SST has the greater effect on CO_2 fluxes (WOLF et al., 2016).

Figure 5.3 - a) Ocean-atmosphere CO_2 fluxes (CO_2 Flux) (µmol m^{-2} s^{-1}), b) Sea Surface Temperature (SST) (°C) and, c) Sea Surface Salinity (SSS) with Po/V H41 route at Brazil Malvinas Confluence from 14 to 27 October of 2018.

a) b) c)

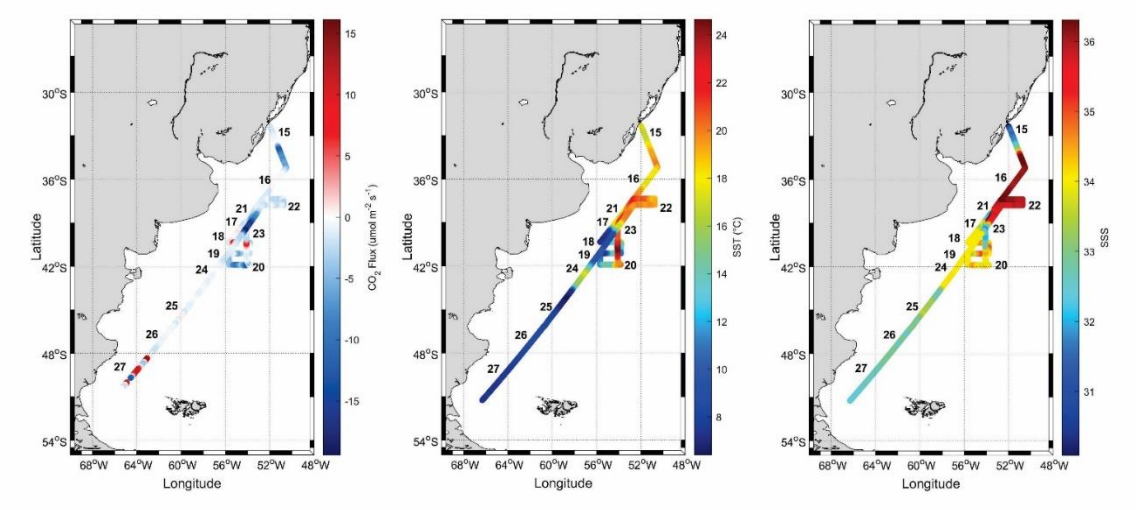

Source: Author's production.

Figure 5.4 – Mean sea level pressure (blue lines), wind direction (arrows) and Po/V H41 location (black point) during the days 16, 21, 22, 24 and 25 October 2018, 00H for each day. Data from ERA 5.

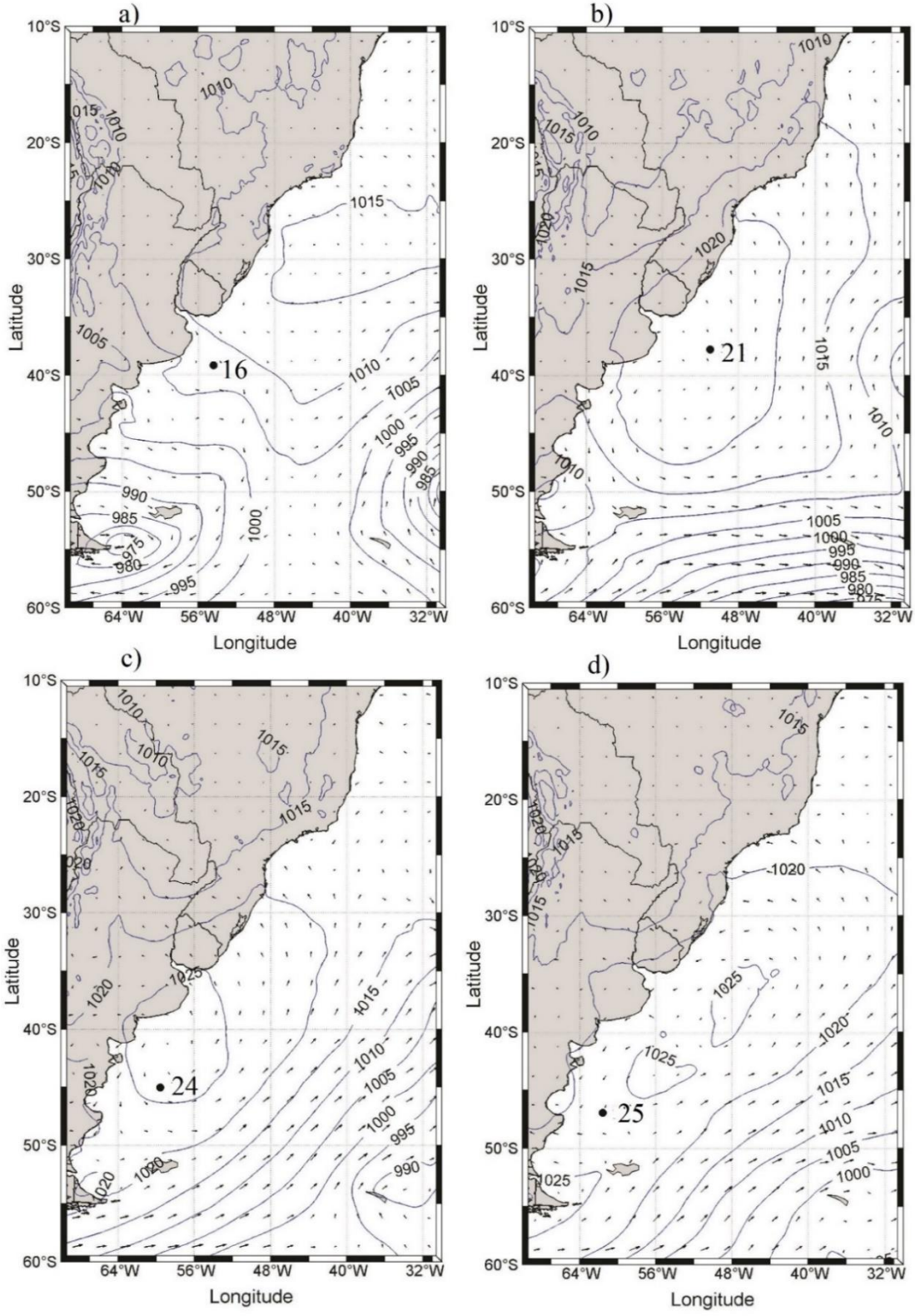

Source: Author's production.

In the beginning of October 23, 2018, a large CO_2 sink was observed in the MC because of the fresh, cold water which increased the solubility of CO_2 in the ocean, along with a high wind speed of approximately 20 m s^{-1}, turbulence greater than approximately 0.5 m s^{-1}, and the presence of chl (Figure 5.2). Thus, the CO_2 flux was directed to the ocean. However, until October 25, 2018, CO_2 fluxes at MC were close to zero owing to the proximity of the ship to high-pressure systems, weak winds at the surface (Figures 5.2a, 5.3c and 5.3d), and low turbulence, thus inhibiting the mass exchange between the ocean and atmosphere. According to Bianchi et al. (2005), the CO_2 sink south of 48° S is not as strong as that in the northern region in the South Atlantic Ocean during spring. However, between October 26 and 27, 2018, the ocean behaved as a CO_2 source, mainly because of the high turbulence in the layer, which intensified mass exchange between the ocean and atmosphere (Figure 5.2). Gonçalves and Innocentini (2018) reported that turbulence increases mass exchange between the ocean and atmosphere. During the cruise, the MC behaved as a CO_2 sink with an average value of -0.48 µmol of CO_2 m^{-2} s^{-1}, with cool and fresh waters, average 9.01 °C and 33.13, respectively (Table 5.1). Similar results were obtained by Padin et al. (2010), who found that MC behaved as a CO_2 sink in spring because of the low SSS value of 32.9. Therefore, atmospheric variables modulate the CO_2 exchange between the ocean and atmosphere.

5.2.2 Vertical analysis

Figure 5.5 presents a synoptic snapshot of the thermal structure of the MABL and ocean mixed layer produced at the BMC between October 16 and 17, 2018. The expendable bathy-thermograph data were used only to describe the main water temperature distribution along the BMC transect, which is important for the MABL analysis. The figure shows the thermal contrast between the warm waters from the BC (red color), with a thermocline of 400 m and 18 °C, and the cold water from MC, with a thermocline of 50 m and 8 °C. Over the warm BC waters, the atmosphere is warmer and presents weaker winds at the sea surface. However, in this study, the MABL was not always well-mixed (unstable) with a small vertical wind shear over warmer waters, as classically

expected for SST forcing through the static stability mechanism (WALLACE et al., 1989). Pezzi et al. (2016) found similar behavior in their investigation of the influence of the cross-shelf oceanographic front occurring between the BC and BCC on the local MABL. They associated the differences from the classical adjustment models with the presence of cyclogenesis and atmospheric frontal passages in their study area. In the well-known vertical mixing mechanism, air buoyancy and turbulence intensity increase over warm waters (PEZZI et al., 2005; 2009; 2021). Consequently, the MABL vertical wind shear is reduced, and stronger winds are generated at the sea surface (PEZZI et al., 2021). The differences from the classical adjustment models are a consequence of the presence of high pressure in our study area, which inhibited the MABL convective process owing to the subsidence of the air to the near surface.

Figure 5.5 - Temperature profiles (°C) of the atmosphere and ocean (colors) taken simultaneously by radiosondes and XBTs along the Brazilian Navy Polar Vessel (Po/V) Almirante Maximiano (H-41) route while crossing the Brazilian Malvinas Confluence between 16 and 17 October 2018.

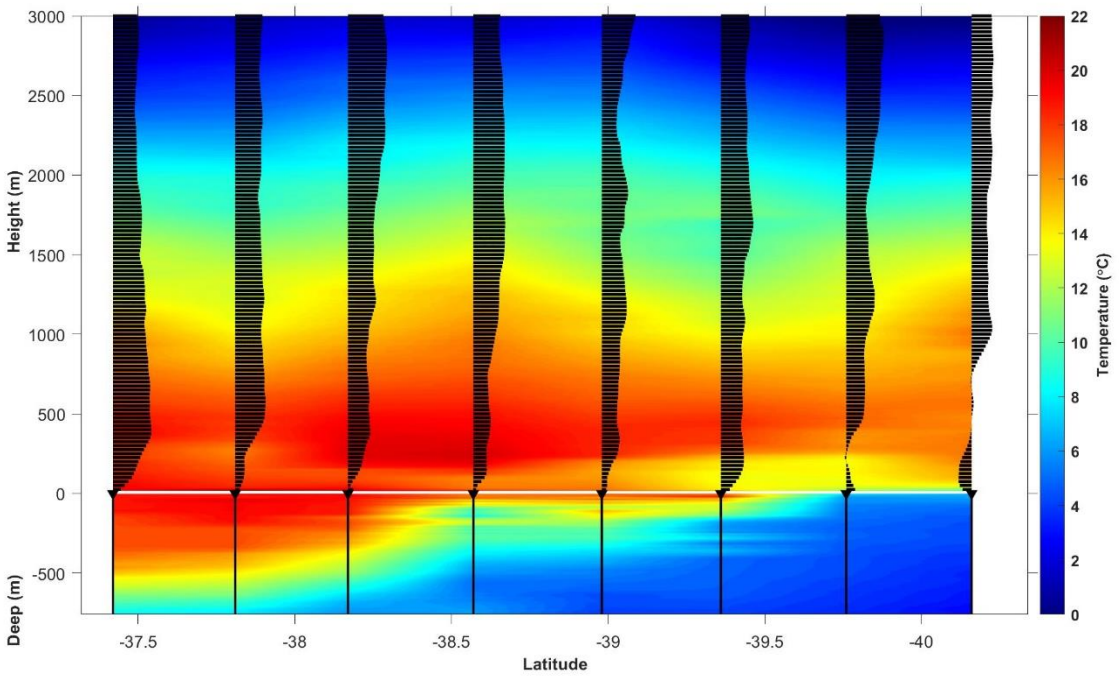

The lower part of this figure displays the oceanic sounding positions (black vertical lines). Wind magnitude (m s^{-1}) in vectors is also displayed, superimposed on the air temperature. The vector size reflects the wind magnitude.
Source: Author's production.

Over cold MC waters, the MABL is not well-developed and has a weak wind at the surface (Figure 5.5). The MABL is stable as the wind shear increases and surface wind decreases, which agrees with the vertical mixing mechanism (WALLACE et al., 1989). Pezzi et al. (2021) identified the impact of the eddy on the turbulent fluxes and its surrounding environment, such as the dynamic and thermodynamic characteristics of the MABL. They found that the mechanisms of pressure adjustment and vertical mixing that could make the MABL unstable were both identified.

Figures 5.6a and 5.6b show the CO_2 flux and stability parameter represented by SST and T_{air}, and CO_2 flux and u*, respectively, during October 16, 2018. The atmosphere was close to neutral conditions at the warm side of the BC with some peaks of instability and low turbulence (<0.4 m s^{-1}). The factors associated with the high-pressure system modulated the CO_2 flux and inhibited the intense mass exchange between the ocean and the atmosphere; the area behaved as a mild CO_2 sink. Under the influence of the MC atmosphere, the BMC was stable above the cold waters (Figure 5.5); however, it had increased turbulence owing to the intense SST gradients, which increased the turbulence and CO_2 flux between the ocean and atmosphere.

Figure 5.6 - a) Sea Surface Temperature (SST) (°C), Air Temperature (T_{air}) (°C), and CO_2 Flux (μmol $m^{-2}s^{-1}$) b) Friction velocity (u*) (m s^{-1}). Values obtained along the ship while crossing the Brazilian Malvinas Confluence between 16 and 17 October 2018.

a)

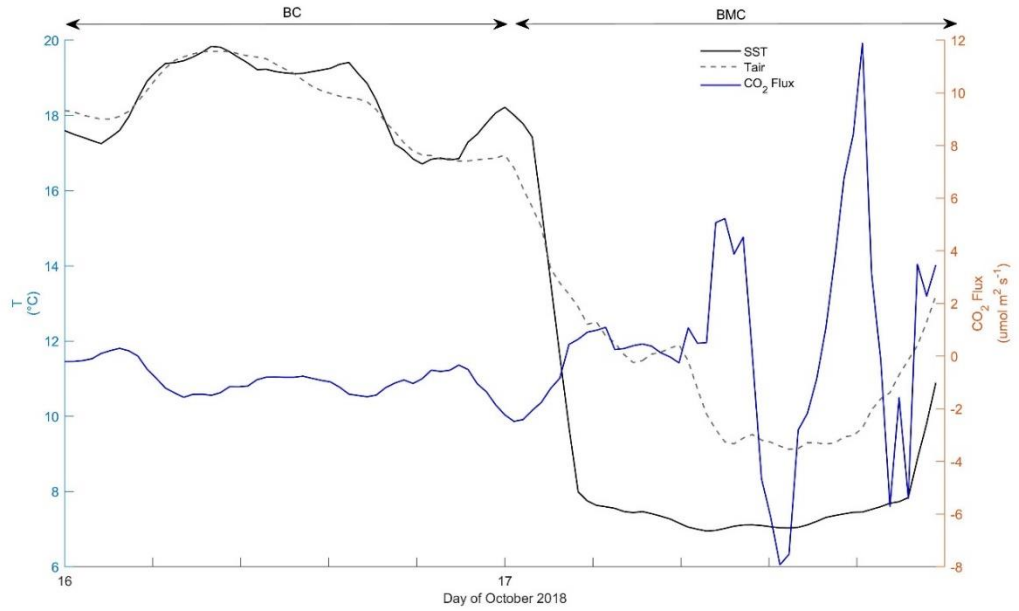

b)

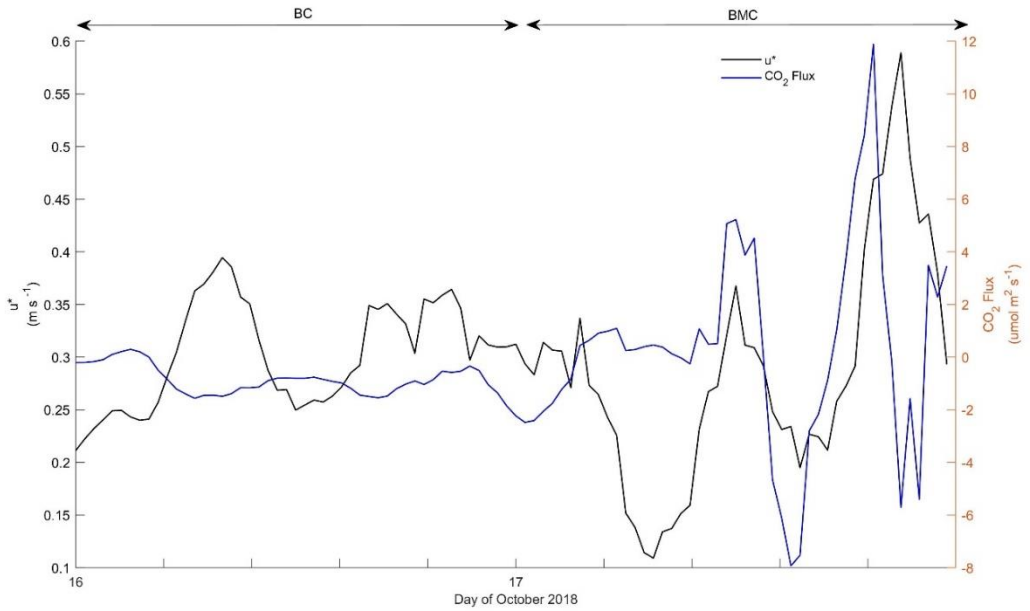

Source: Author's production.

5.3 Conclusions

This study showed the impacts of different atmospheric and oceanic conditions on the ocean-atmosphere CO_2 flux exchange based on a combination of *in-situ*, satellite, and reanalysis data. The *in-situ* data were collected during one scientific cruise on board a polar vessel that is part of a Brazilian scientific effort called the ATMOS Project. The *in-situ* data were collected in the Southwest Atlantic Ocean during the first phase of Antarctic Operation 37, covering October 14–27, 2018. The CO_2 fluxes were obtained using the eddy covariance method (MILLER et al., 2008; PEZZI et al., 2021). Oceanic conditions were analyzed using chl, SSS, and SST data from satellites. The atmospheric synoptic conditions were obtained through the ERA5 reanalysis dataset by analyzing the air temperature, sea level pressure, wind speed, and direction.

CO_2 fluxes exhibit complex behavior at the ocean-atmosphere interface because they are modulated by different oceanic and atmospheric conditions. The BCC behaved as a sink because of the high chl concentration and fresh water, which directed the fluxes to the ocean. In this layer, biochemical parameters, such as chl and SSS, rather than SST, modulate CO_2 flux. The BC was the area with the highest CO_2 absorption during the study period. This result is mainly because of the proximity to the chl-rich and less saline waters of La Plata River and to the cold and fresh waters of the MC. Moreover, this is owing to the intense wind speed, which increases the CO_2 flux between the ocean and atmosphere. On average, the BMC behaved as a CO_2 sink, and the modulation of CO_2 fluxes was due to the intense horizontal gradient of SST combined with moderate wind and turbulence, which contributed to the mass exchange between the ocean and atmosphere. The MC sequestered less carbon than the BC and BMC because of the proximity of the ship to high-pressure systems coupled with low turbulence and light winds on the surface that inhibited the exchange of mass between the ocean and atmosphere.

The MABL over the BMC, on the cold side of the MC waters, had weak winds at the surface and a highly stable MABL, supporting the existence of MABL modulation by the vertical mixing mechanisms. However, on the warm side from

the BC waters, the MABL was more developed, but the wind was not strong and wind shear was present. In this case, the MABL was modulated by the high-pressure system, which decreased turbulence. However, the intense mass exchange between the ocean and atmosphere was inhibited, and the area behaved as a light CO_2 sink because of the high-pressure system.

These results demonstrate that atmospheric and oceanic conditions modulate CO_2 fluxes between the ocean and atmosphere. The collection of *in-situ* data is fundamental to improving our knowledge of the mass exchange between the ocean and atmosphere. Data collection efforts in this region should be continued to expand our knowledge of the importance of the Southwest Atlantic in the global carbon balance.

6 DIRECT AND INDIRECT MEASUREMENTS OF CO_2 TURBULENT FLUXES IN THE SOUTHWEST ATLANTIC OCEAN

6.1 Introduction

The ocean acts as a major sink of CO_2 soaking up about 25%-48% of the total anthropogenic emissions (SABINE et al., 2004; CANADELL et al., 2007; DONEY et al., 2009, TAKAHASHI et al., 2009; LE QUERE et al., 2018). There are several methods for quantifying carbon flux between the ocean and the atmosphere (MILLER et al., 2010; TAKAHASHI et al., 2009; FARIAS et al., 2012). One of them is the direct method, eddy covariance (EC), which obtains mass and energy turbulent fluxes, between the surface and the atmosphere, by using micrometeorological instrumentations (BUTTERWORTH; MILLER, 2016). There is also the indirect method called bulk parameterizations, based on characteristics of the air–sea interface (KARA et al., 2000), formulations based on empirical parameterization of turbulence (FAIRALL et al., 1996).

However, those indirect estimations result in uncertainties about the CO_2 balance in the ocean-atmosphere system (PEZZI et al., 2015). The estimation of ocean CO_2 uptake is still biased by the uncertainty of parameterization of gas transfer velocity (K). The K coefficient is considerate the major source of uncertainty in the Bulk methodology. The K is traditionally estimated using wind speed because it is considered an indirect parameter for the ocean surface roughness (PHILLIPS, 1977), which is a fundamental role in gas exchange. Despite bulk research on this subject, our perception of the gas transfer processes remains to be enhanced. However, other processes are also important, such as boundary layer instabilities and wave parameters, which are not affected solely by wind speed (WOOLF et al., 2005; 2007; ZHAO et al., 2003). In addition, there is a need to integrate the chemical, physical and biological knowledge, which are essential to the CO_2 exchange processes (BRÉVIÈRE et al., 2015; NEUKERMANS et al., 2018).

Understanding how CO_2 turbulent flux exchange behaves in different oceanic regions is very important for assessing the global carbon budget. The CO_2 partial pressure (pCO_2) in the ocean has great spatial and temporal variability,

especially at the middle and high latitude regions, considered CO_2 sinks (TAKAHASHI et al., 2009). The spatial distribution and temporal variability of pCO_2 have not yet been fully comprehensively in the southwestern Atlantic Ocean. The *in situ* fCO_2 data have gaps in coverage spatial and temporal resolution (TAKAHASHI et al., 2009; CARVALHO et al., 2018; LENCINA-AVILA et al., 2016). There is a need for improving our understanding of the processes involved in the exchange between the ocean and the atmosphere, particularly at different spatiotemporal scales. The *in situ* data is typically collected in the summer, which makes it a scientifically complex environment for experimentation, due to its distance, hostility and adverse nature (PEZZI et al., 2021; MONTEIRO et al., 2020). To solve this issue, there is regional climatology of sea surface fCO_2 (TAKAHASHI et al., 2018), or algorithms developed from the hydrographic or carbonate system datasets (ITO et al., 2016; LENCINA-AVILA et al., 2016; BENALLAL et al., 2017; ORSELLI et al., 2019a). Those algorithms allied to satellite data can increase the spatial and temporal resolution of the sea surface fCO_2 distribution (ZHU et al., 2009; BENALLAL et al., 2017). Which improve our knowledge of the role of the SAO in the global climate (SHUTLER et al., 2016; BENALLAL et al., 2017; WANNIKHOFF et al., 2017; LOHRENZ, et al., 2018). Changes in the sea surface fCO_2 are associated to sea surface temperature (SST), sea surface salinity (SSS), total alkalinity (Alk), and total dissolved inorganic carbon (DIC) (SIGNORINI et al., 2013).

The CO_2 flux between ocean and atmosphere is quite complicated because it needs knowledge of ocean physics, atmospheric physics, cloud physics, and chemistry, as well as biogeochemical cycles in general (ITO et al., 2018; MONTEIRO, et al., 2020; JIANG et al., 2014). The Atlantic Ocean is the most important CO_2 sink, providing about 60% of the global ocean uptake of the global anthropogenic CO_2 uptake from the atmosphere from 1870 to 1995 (TAKAHASHI et al., 2009; FRÖLICHER et al., 2015; LE QUÉRÉ et al., 2016, 2018). The Southwest Atlantic Ocean plays a major role in the weather and climate of the south and southwestern areas of Brazil and other South American countries (PEZZI et al., 2015).

The main objective of this work is to purpose a gas transfer coefficient for the Southwest Atlantic Ocean based on *in situ* data collected at that region. Furthermore, we will validate the gas transfer coefficient for other fields campaigns. Also, it will be used this transfer velocity coefficient to estimate a CO_2 flux with bigger spatiotemporal resolution for the region.

6.2 Results and discussion

The results are composed by the algorithm for the determination of the fCO_{2sw} for the study region. Also, the comparisons between the calculated FCO_2 with *in situ* (EC) and with the Bulk methodology with different gas transfer velocity, developed by several researchers. Furthermore, the purposed gas transfer coefficient for the study area. For validation of the fCO_{2sw} and K was made by the comparisons between FCO_2 flux computed results and field measurements taken during the oceanographic cruises where EC was used. The last part was the climate variability of CO_2 flux between ocean and atmosphere for the study region.

6.2.1 CO_2 fugacity at ocean

The fugacity of carbon dioxide is not the same as its partial pressure (the product of mole fraction of CO_2 and total pressure), but rather takes account of the non-ideal nature of the gas phase (WEISS 1974; DOE, 1994). According to the the fugacity and partial pressure of CO_2 differ by only about 0.4 % (LISS; JOHNSON, 2014).

The fCO_{2sw} model was created with SST and fCO_{2sw} data from SOCAT for the OP37 (Figure 6.1). We found the best fit was $fCO_{2sw} = 0.3181*SST^2 - 9.51*SST + 397.9$ with R^2 of 0.64 at 95 % of confidence. Different results were found for Benallal et al. (2017), which found a better model using the feedforward neural networks, for the Southern Ocean from the south of Australia to the Antarctica coasts based on SST and chl. Zhu et al. (2009) found a better fit for fCO_{2sw} with SST and chl, for the northern China Sea, because it is a more productive area and closer to the coast than our study area.

Figure 6.1 - Linear regression between SST and fCO_{2sw} during the OP37, for the period from October to November 2018.

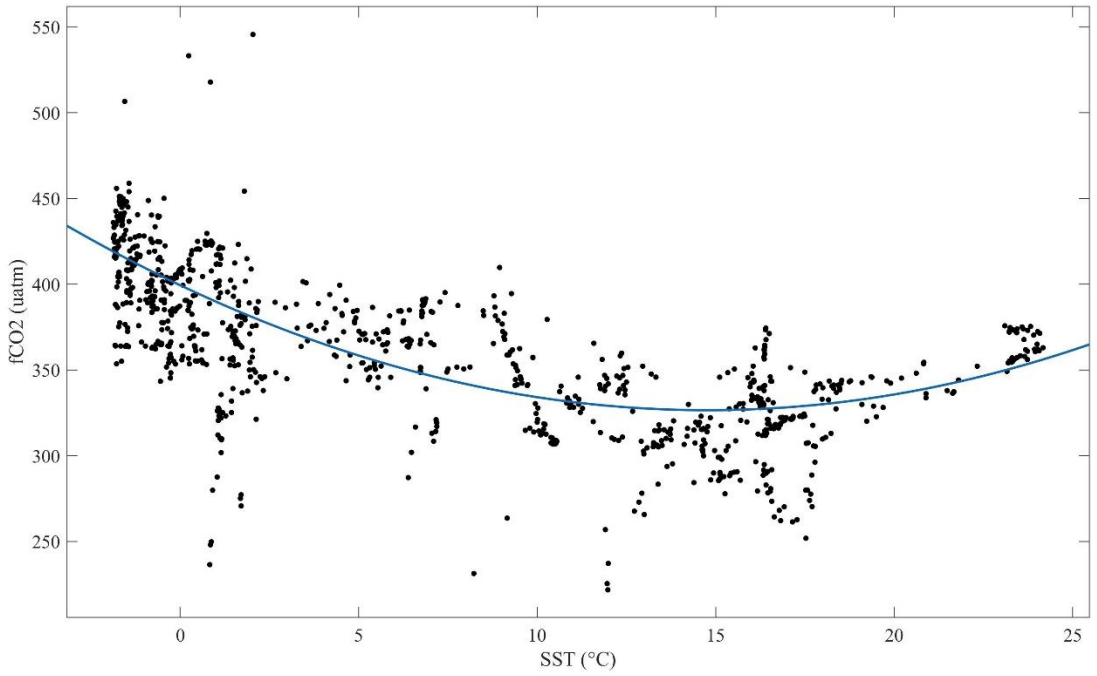

Source: Author's production.

6.2.2 Gas transfer coefficient

Several researchers have developed the gas transfer velocity since 1980s for different regions in the World Ocean and environmental conditions. In this study, we tested the most used equations, which are based on wind speed (Table 6.1), for OP37. Table 5 presents a comparison between the calculated FCO_2 with both *in situ* (EC) and with the Bulk methodology. The results were similar for all models, with RMSE between 5.95 to 7.43 and Pearson correlation between 57 and 74% at the 95% confidence level. The best equation was Wanninkhof (1992), which includes the chemical effects and the exchange between ocean and atmosphere. Pezzi et al. (2021) equation show good correlation as well, however the coefficient was developed including eddy effects.

Table 6.1 - Model results for CO_2 flux using different gas transfer velocities for OP 37.

Reference	RMSE	PEARSON
Wanninkhof (1992)	7.44	0.75
Wanninkhof and McGillis (1999)	6.09	0.69
Nightingale et al. (2000)	6.11	0.57
Jean-Baptiste, Fourré, and Poisson (2002)	7.02	0.62
Ho et al. (2006)	6.13	0.59
Sweeney et al. (2007)	5.92	0.67
Wanninkhof et al. (2009)	6.10	0.59
Ho et al. (2011) (Equation (a))	5.96	0.67
Ho et al. (2011) (Equation (b))	6.12	0.69
Wanninkhof (2014)	6.08	0.60
Pezzi et al. (2021)	6.39	0.61

Source: Author's production.

The EC is considered the best method to quantify the ocean–atmosphere CO_2 fluxes because its uncertainties are of the order of only 5% (DONG et al., 2021). These uncertainties are much smaller than those associated with the bulk methods that use (uncertain) parameterized transfer coefficients. The ocean–atmosphere CO_2 transfer velocity coefficient, computed with our data and quadratically fitted to wind speed, yielded good performance by agreeing with K determined in other CO_2 studies as shown in Figure 6.2.

In order to assess the quality of the CO_2 fluxes calculated in this study, the CO_2 ocean–atmosphere transfer velocity coefficient (K) was computed and compared to some classic values found in the literature (Figure 5.4). We found a quadratic adjustment ($K = 0.2325*u^2 – 0.4361*u + 1.764$ with R^2 of 0.97 and 95 % of confidence) between the CO_2 transfer coefficients and the neutral wind speed collected at 10 m during the cruise. For u less than 5 m s^{-1} our curve showed a good agreement with Wanninkhof (1992) and Pezzi et al. (2021) for less than 10 m s^{-1} good agreement with Wanninkhof and McGillis (1999) and Ho et al. (2011) (Equation (b)). However, for u greater than 5 and 10 m s^{-1}, the K values were lower than those curves used for comparison. Even so, it is possible to observe that the K curve was able to well represent the expected behavior compared to the other curves, but for the winds bigger than 15 m s^{-1}, values are higher compared to those curves. When the wind speed is zero then K = 1.764 cm h^{-1}, which is higher than most of the studies used here for comparison. However, it is smaller than the Wanninkhof et al. (2009), which the wind is zero, K= 3 cm h^{-1}. We can associate this value to the turbulence processes at the ocean surface (intense horizontal SST gradients) or the biological activity (waters from the Rio del Plata) that is characteristic of this region. The BMC has an important natural contributor to the atmospheric carbon budget throughout their intense SST gradient.

Figure 6.2 - Relationship between the CO_2 transfer velocity coefficient and the neutral wind speed at 10 m calculated from the data collected in this experiment.

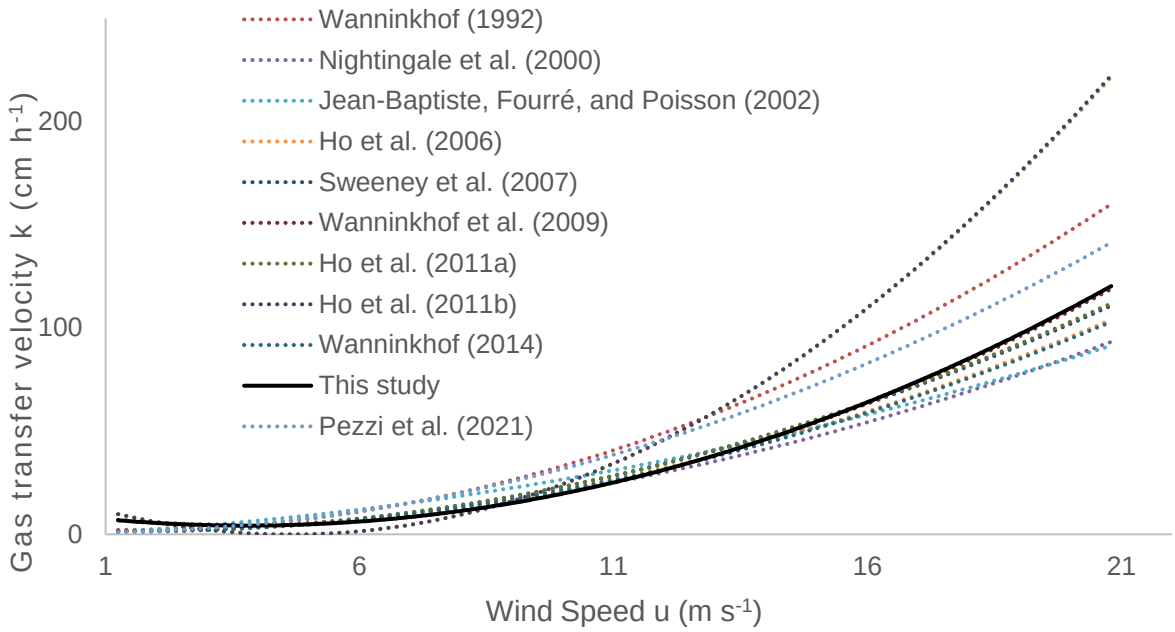

Source: Author's production.

6.2.3 Validation

Satellite and reanalysis data were used at SAO for computing CO_2 flux using the bulk methodology using the estimated parameters, fCO_{2sw} and K. Comparisons were made between computed results and field measurements taken during the oceanographic cruises where EC was used. We used ACEX data (2012), OP 32, 33, 34 and 37 (2013, 2014, 2015, and 2018, respectively), for the SAO. The results shown RMSE between 2.64 to 8.17 and Pearson correlation between 54% and 85% at the 95% confidence level (Table 6.2). The ACEX campaign has the lowest correlation and highest RMSE, due to the location of the route, more to the north and near to the coast, in the Brazil Coastal Current (BCC). The others had similar statistical results because they have similar routes. Thus, they crossed Brazil current (BC), Brazil-Malvinas Confluence (BMC) and Malvinas current (MC). This suggests the effects of

biological activities on the spatial and temporal changes in FCO_2 in the BCC cannot be ignored, and an algorithm dependent on both SST and chl is a better fit for the target region. However, the fCO_{2sw} and transfer velocity algorithms have satisfactory results when compared to *in situ* data.

Further optimization of this algorithm based on a larger pool of *in situ* data is nevertheless advocated. Nevertheless, there are significant discrepancies between each pair of data, due mainly to the differences in the time and spatial scales of remote sensing, reanalysis and *in situ* data. The remote-sensing and reanalysis data used here are on hourly, daily, weekly and monthly time scales, while the temporal resolution of the *in situ* data was obtained at high frequency as 20 data per second. Also, the spatial resolution for satellite and reanalysis data varies between 2.2 x 2 km to 0.25°. It is clear, that the relatively drastic short-term changes in FCO_2, such as high frequency variability or even the diurnal cycle variability, cannot be captured in the remote-sensing and reanalysis data. Furthermore, the different spatial and temporal resolution between remote sensing / reanalysis and *in situ* data do not affect the comparison between different algorithms.

Table 6.2 - Comparison between FCO_2 between ocean and atmosphere, calculated with *in situ* data (eddy covariance) and with the satellite / reanalysis data (*bulk* methodology) with the estimated parameters fCO_{2sw} and K.

Ship campaign	Statistical
ACEX (2012)	RMSE= 8.17 R^2= 0.54
OP 32 (2013)	RMSE= 4.85 R^2= 0.74
OP 33 (2014)	RMSE= 7.29 R^2= 0.73
OP 34 (2015)	RMSE= 7.81 R^2= 0.67
OP37 (2018)	RMSE= 2.64 R^2= 0.85

The *in situ* data used were ACEX (2012), OP 32 (2013), OP 33 (2014), OP 34 (2015) and OP 37 (2018).

Source: Author's production.

6.2.4 Climate variability

The time series analysis shown in Figure 6.3, reveals some interesting CO_2 behavior along the years. The BC and MC had been increasing the assimilation of carbon (Figure 6.3) along the analyzed years. The Figure 5 show negative anomaly between 2012 and 2020 for CO_2 flux and SSS. The negative tendency in SSS may contributed to the increased sink of CO_2 sink by the ocean, due to the increase CO_2 solubility. However, the SST in BC and MC presented almost neutral tendency. The chl has a week positive tendency, it could contribute for the CO_2 flux negative anomaly. Allied to that, the salinity had more impact on the CO_2 flux than SST between January of 2003 and December of 2020.

Figure 6.3 - CO_2 flux anomaly (FCO_2 flux anomaly), sea surface temperature anomaly (SST anomaly), sea surface salinity anomaly (SSS anomaly) and chlorophyll anomaly (chl anomaly), during January 2003 and December 2020.

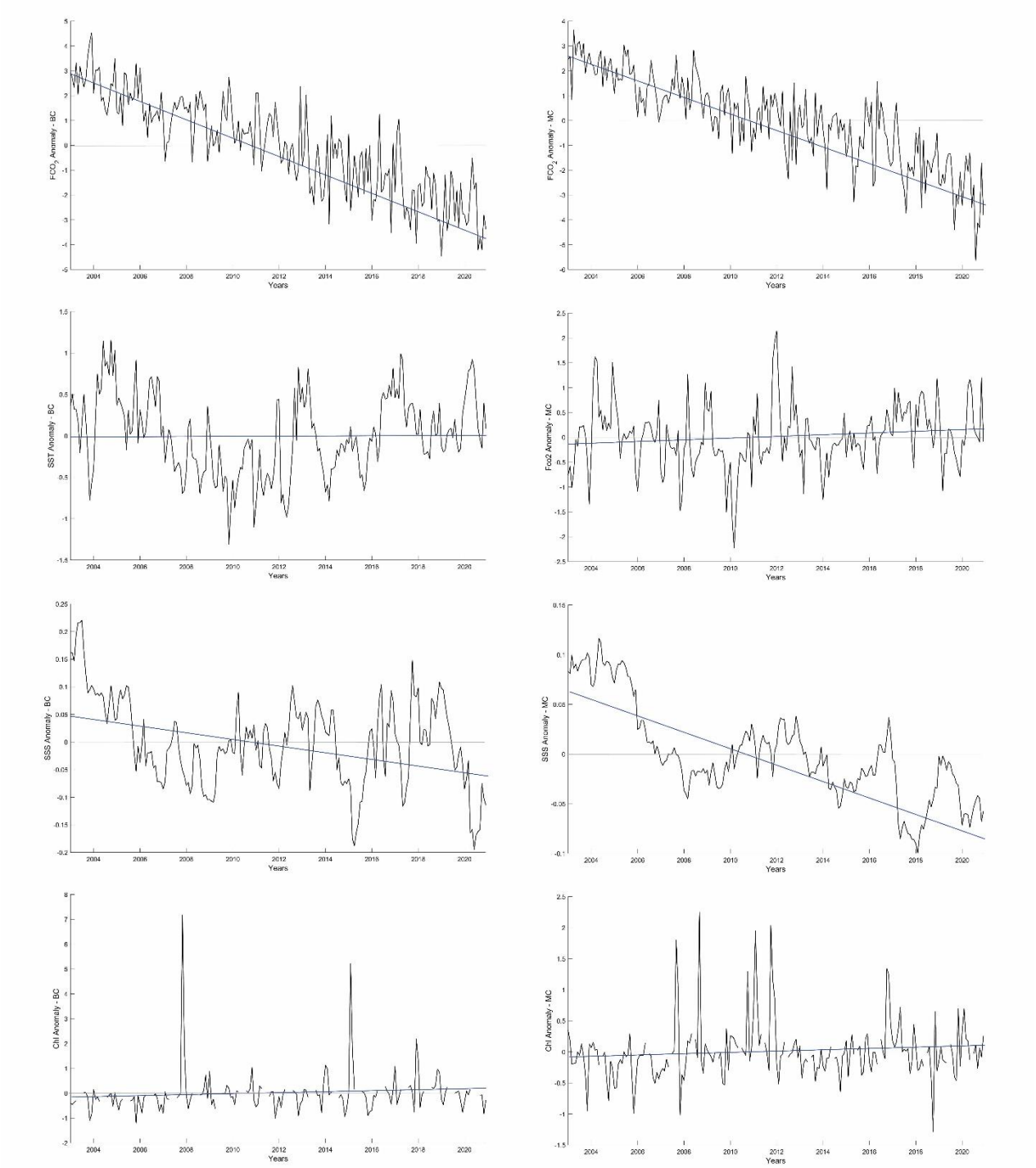

Source: Author's production.

Furthermore, the CO_2 concentration in the atmosphere has increased 9% between 2003 and 2020. This consistent increased of CO_2 in the atmosphere, may have directed the CO_2 to the ocean, due to the difference of partial pressure of carbon dioxide between ocean and atmosphere. Similar results were found by Benallal et al. 2017, for the Southern Ocean that has becomes a stronger sink of CO_2 throughout the years, from an overall average absorption of about 2 mmol CO_2 m^{-2} day^{-1}in 2002/2003 to about 7 mmol CO_2 m^{-2} day^{-1} in 2014/2015. According to the authors, the persistent increase of fCO_{2sw} in the atmosphere make the region absorbing more and more atmospheric CO_2, which may probably lead to ocean acidification in this area.

The anomaly of the *in situ* and climatology data for the OP37 are show in Figure 6.4, from where we can see the positive values for CO_2 flux and SST. However, SSS anomaly display negative values in the MC and positive values in the BC. Thus, the SST modulates the CO_2 flux direction. The region absorbed less CO_2 than the climatology, especially because of the high-pressure atmospheric system that was present at the moment, which inhibit the exchange of mass between ocean and atmosphere. The high pressure in the OP37 contributed to modulated CO_2 flux, which was responsible for the difference between the OP 37 and the climatology, which was not capture in the bulk methodology.

Figure 6.4 - CO_2 flux anomaly (mmol m^{-2} d^{-1}), sea surface temperature anomaly (SST anomaly) (°C), sea surface salinity anomaly (SSS anomaly), for the OP37 compared with the climatology data (October of 2003 to 2020).

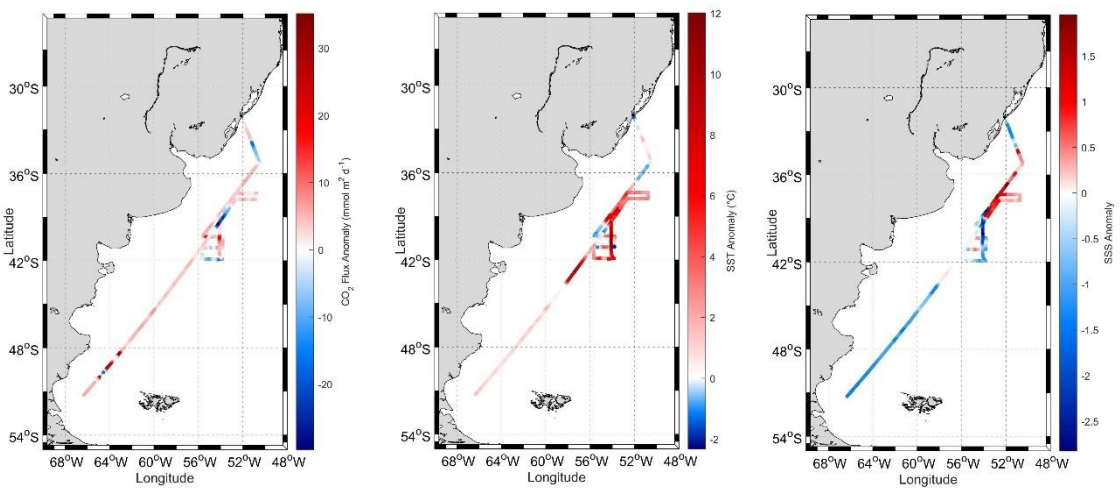

Source: Author's production.

The analyzed region shows a marked seasonal variability, acting more as a CO_2 sink during the winter and spring, as shown in Figure 6.5). The same results were found by Takahashi et al. (2009), where in their study in the South Atlantic (14S to 50S) sank more CO_2 during August to November. However, the entire area behaved as a CO_2 sink for the 4 seasons, the same behavior was found by Takahashi et al. (2009). According to the Bianchi et al. (2009) the Southwest Atlantic Ocean is one the most important area for CO_2 sink in the world, with an average of -3.7×10^{-3} mol C m^{-2} d^{-1}. During the summer the north of 40° sink less CO_2 than other seasons, due to the increase of SST, which reduces the CO_2 solubility in the ocean, thus it reduces CO_2 sink. Similar results were found by Bianchi et al. (2009), the region between the 39 to 43 °S closer to the coast reduced the sink of CO_2 flux about 20% in the area, due to the increase SST and pCO_2 in the ocean.

Figure 6.5 - CO_2 flux distribution during Spring, Summer, Autumn and Winter in the Southwest Atlantic Ocean for the period between January 2003 and December 2020.

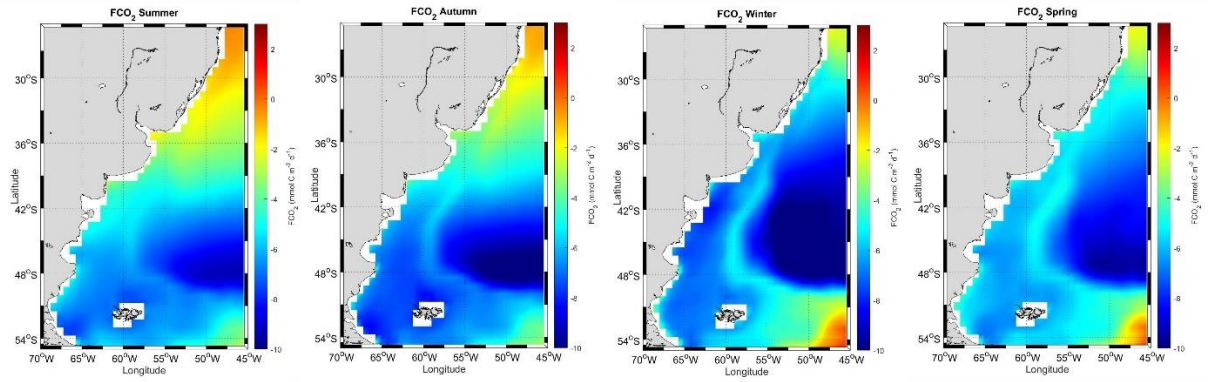

Source: Author's production.

6.3 Conclusions

- The fCO_{2sw} modeled using SST data, has satisfactory performance in the Southwest Atlantic Ocean.
- The ocean–atmosphere CO_2 transfer velocity coefficient, computed with our data and quadratically fitted to wind speed, yielded good performance by agreeing with K determined in other CO_2 studies.
- The bulk methodology for CO_2 flux between ocean and atmosphere, using the two parameterization fCO_{2sw} and K, had a good agreement with the *in situ* data (eddy covariance) for the Southwest Atlantic Ocean.
- The BC and MC had been increasing the assimilation of carbon along the years analyzed (2003 to 2020). This increasing of assimilation is mainly due to the increase of CO_2 concentration in the atmosphere, allied to the negative tendency of SSS.
- The anomaly between *in situ* data for October 2018 and climatology data (2003 to 2020), shows that the SST anomaly modulates the CO_2 flux between Ocean and atmosphere. Also, during the route has high pressure system, which inhibited the flux between ocean and atmosphere. The discrepancy between CO_2 flux for OP37, using *in situ*

data with eddy covariance and the climatology data, using bulk methodology is related to the different temporal and spatial resolution.

- The seasonal variability in CO_2 flux shows the Southwest Atlantic Ocean sink more CO_2 during winter and spring.

7 FINAL REMARKS

There are many aspects that could be enhanced for CO_2 flux with *in-situ*, satellite and reanalysis data. For *in-situ* data, which is used in eddy covariance for CO_2 flux calculation, should have more data collection during the year, which could expand the knowledge of CO_2 behavior in seasonal studies with high resolution. However, it is comprehensively the difficult access in the Southern Ocean, due to the distance and adverse nature. For the satellite and reanalysis data, that need to apply the bulk methodology, could improve if we have more *in-situ* data such as wave parameters and biochemical parameters for the development of more robust gas transfer velocity and CO_2 fugacity parameter.

We were able to focus on the *in-situ* data collected in Spring and Summer of each field campaign and in the bulk methodology validated with those *in-situ* data. Furthermore, our findings highlighted the importance of the of collection of *in-situ* data to improving our knowledge of the CO_2 exchange behavior in the Southwest Atlantic Ocean and Southern Ocean. We also highlighted the importance of satellite, reanalysis, and *in-situ* data combinations for improve the understanding of CO_2 flux between ocean and atmosphere. The CO_2 fluxes exhibit complex behavior at the ocean-atmosphere interface because they are modulated by different oceanic and atmospheric conditions. The Malvinas Current sank less CO_2 than Brazil Current and Brazil Malvinas Confluence in the OP 37, even though it has more cold and fresh water. This behavior was due to the high-pressure system and stable atmosphere, which inhibited the CO_2 flux. The Bransfield Strait uptake 38.59% more CO_2 than the Drake Passage due to the cold and fresh waters, allied to the influence of glacial meltwater dilution. Moreover, the study was conducted during a positive and active phase of the SAM and El Niño, which could influence the area behaved as CO_2 sink. The Southwest Atlantic Ocean is sinking more CO_2 flux along the years due to the increasing of CO_2 concentration in the atmosphere may probably lead to ocean acidification in this area.

It is very important to maintain the *in-situ* datasets and improve the sampling methods for evaluating the performance of the satellite and reanalysis data. Thus, the effort to keep long-term *in situ* sampling is essential for monitor CO_2

exchange behavior and produce reliable information for decisions about mitigating climate change.

REFERENCES

ARYA SP. **Introduction to micrometeorology**. USA: Academic Press, 2001.

ARRUDA, R. et al. Air-sea CO2 fluxes and the controls on ocean surface pCO2 seasonal variability in the coastal and open-ocean southwestern Atlantic Ocean: a modeling study. **Biogeosciences**, v.12, p. 5793–5809, 2015.

BARLLET, E. M. R. et al. On the temporal variability of intermediate and deep waters in the western basin of the bransfield strait. **Deep Sea Research,** v.149, p. 31-46, 2018.

BAKKER, D.C.E. et al. A multi-decade record of high quality *f*CO2 data in version 3 of the Surface Ocean CO2 Atlas (SOCAT). **Earth System Science Data**, v. 8, n. 2, p. 383–413, 2016.

BENALLAL, M. A. et al. A. Satellite-derived CO2 flux in the surface seawater of the Austral Ocean south of Australia. **International Journal of Remote Sensing**, v. 38, n. 6, p. 1600–1625, 2017.

BIANCHI, A. A. et al. Annual balance and seasonal variability of sea-air CO2 fluxes in the Patagonia Sea: their relationship with fronts and chlorophyll distribution. **Journal of Geophysical Research**, v.114, 2009.

BRÉVIÈRE, E. et al. Surface ocean-lower atmosphere study: Scientific synthesis and contribution to Earth system science. **Anthropocene**, v. 11, 2015.

BROWN, M. S. et al. Enhanced oceanic CO2 uptake along the rapidly changing West Antarctic Peninsula. **Nature Climate Change**, v. 9, p. 678-683, 2019.

BUTTERWORTH, B. J.; MILLER, S. D. Automated underway eddy covariance system for air-sea momentum, heat, and CO2 fluxes in the Southern Ocean. J**ournal of Atmospheric and Oceanic Technology,** v. 33, p. 635-652, 2016.

CAETANO, L.S. et al. High-resolution spatial distribution of p CO2 in the coastal Southern Ocean in late spring. **Antarctic Science**, v. 32, n. 6, p. 476–485, 2020.

CAMARGO, R.; TODESCO, E.; PEZZI, L. P.; SOUZA, R. B. Modulation mechanisms of marine atmospheric boundary layer at the Brazil-Malvinas Confluence region. **Journal of Geophyiscal Research Atmosphere**, v. 118, n. 12, p, 6266–6280, 2013.

CAMPBELL SCIENTIFIC INC. **IRGASON integrated CO2 and H2O open-path gas analyzer and 3-D sonic anemometer**. [S.l.]: Campbell, 2016.

CAMPOS, E. J. D. O papel do oceano nas mudanças climáticas globais. **Revista USP**, v. 103, p. 57-66, 2014.

CANADELL, J. G. et al. Contributions to accelerating atmospheric CO2 growth from economic activity, carbon intensity, and efficiency of natural sinks. **Proceedings of the National Academic Science**, v. 104, n. 47, p. 18866–18870, 2007.

CARVALHO-BORGES, M. et al. Seawater acidification and anthropogenic carbon distribution on the continental shelf and slope of the western south Atlantic ocean. **Journal of Marine Systems**, v. 187, p. 62–81, 2018.

CARVALHO, A. C. O. et al. Phytoplankton strengthen CO2 uptake in the South Atlantic Ocean. **Progress in Oceanography,** 2020.

CAVALCANTI, I. F.; AMBRIZZI, T. A. T. **Tempo e clima no Brasil**. São Paulo: Oficina de Textos, 2009.

CHELTON, D. B.; SCHLAX, M. G.; WITTER, D. L.; RICHMAN, J. G. Geosat altimeter observations of the southern of the surface circulation ocean data. **Journal of Geophysical Research**, v. 95, p. 17877–17903, 1990.

COSTA, R. R. et al. Dynamics of an intense diatom bloom in the Northern Antarctic Peninsula, February 2016. **Limnology and Oceanography**, v. 6, p. 1–20, 2020.

DICKSON, A. G.; GOYET, C. **DOE: handbook of methods for the analysis of the various parameters of the carbon dioxide system in sea water**. [S.l.]: ORNL/CDIAC, 1994.

DONG, Y. et al. Uncertainties in eddy covariance air-sea CO2 flux measurements and implications for gas transfer velocity parameterisations. **Atmospheric Chemistry and Physics**, v. 21, n. 10, p. 8089– 8110, 2021.

DONEY, S. C. et al. Surface-ocean co2 variability and vulnerability. **Deep Sea Research Part II: Topical Studies in Oceanography**, v. 56, n. 8/10, p. 504–511, 2009.

EDSON, J. B. et al. Direct covariance flux estimates from mobile platforms at sea. **Journal of the Atmosphere Ocean Technolology**, v. 15, n. 2, p. 547–562, 1998.

EMERSON, S.; HEDGES, J. **Chemical oceanography and the marine carbon cycle**. Cambridge: Cambridge University Press, 2008.

FAIRALL, C. W. et al. Bulk parameterization of air-sea fluxes for tropical ocean-global atmosphere coupled-ocean atmosphere response experiment. **Journal of Geophysical Research: Oceans**, v. 101, n. C2, p. 3747– 3764, 1996.

FARIAS, E. G. G. et al. Variability of air-sea CO2 fluxes and dissolved inorganic carbon distribution in the Atlantic basin: a coupled model analysis. **International Journal of Geosciences**, v. 2013, p. 249–258, 2013.

FAY, A. R. et al. Utilizing the drake passage time-series to understand variability and change in subpolar Southern Ocean pCO2. **Biogeosciences**, v.15, 2018

FRATINI, F. et al. Relative humidity effects of water vapour fluxes measured with closed-path eddy-covariance systems with short sampling lines. **Agricultural Forest Meteorology**, v. 165, p. 53–63, 2012

FOKEN, T. et al. **Post-field data quality control**. Dordrecht, Netherlands: Springer, 2005.

FRÖLICHER, T. L. et al. Dominance of the Southern Ocean in anthropogenic carbon and heat uptake in CMIP5 model. **Journal of Climate**, v. 28, n. 2, p. 862-886, 2015.

FUJITANI, T. Direct measurement of turbulent fluxes over the sea during AMTEX. Pap. **Meteorolical Geophysics**, v. 32, n. 3, p.119–134, 1981.

GONÇALVES, I. A.; INNOCENTINI, V. Analytical quantification of carbon dioxide exchange mediated by spume Ddoplets. **Boundary-Layer Meteorology**, v. 169, n. 2, p. 327–345, 2018.

GRAMCIANINOV, C.B.; HODGES, K. I.; CAMARGO, R. The properties and genesis environments of South Atlantic cyclones. **Climate Dynamics,** v. 53, p. 4115–4140, 2019.

HACKEROTT, J. A. et al. The role of roughness and stability on the momentum flux in the marine atmospheric surface layer: a study on the southwestern Atlantic Ocean. **Journal of Geophysical Research Atmosphere,** v. 123, n. 8, p. 3914–3932, 2018.

HENLEY, S. F. et al. Changing biogeochemistry of the Southern Ocean and its ecosystem implications. **Frontiers in Marine Science**, v. 7, e 581, 2020.

HERSBACH, H. et al. **ERA5 hourly data on single levels from 1979 to present**. [S.l.]: Copernicus Climate Change Service, 2018.

HO, D. T. et al. Measurements of air-sea gas exchange at high wind speeds in the southern ocean: implications for global parameterizations. **Geophysical Research Letters,** v. 33, n. 16, 2006.

HO, D. T. et al. Toward a universal relationship between wind speed and gas exchange: gas transfer velocities measured with 3he/sf6 during the southern ocean gas exchange experiment. **Journal of Geophysical Research**: **Oceans**, v. 116, n. C4, C00F04, 2011.

HOSKINS, B.J.; HODGES, K.I. A new perspective on Southern Hemisphere storm tracks. **Journal of Clim**ate, v. 18, n. 20, p. 4108-4129, 2005.

INTERNATIONAL PANEL ON CLIMATE CHANGE (IPCC). **Climate change 2021: the physical science basis. contribution of working group i to the sixth assessment report of the intergovernmental panel on climate change.** Cambridge: Cambridge University Press, 2021.

ITO, R. G.; GARCIA, C.A.E.; TAVANO, V.M. Net sea-air CO2 fluxes and modelled pCO2 in the South western subtropical Atlantic continental shelf during spring 2010 and summer 2011. **Continental Shelf Research**, v. 119, p. 68–84, 2016.

ITO, R. G. et al. Sea-air CO2 fluxes and pCO2 variability in the Northern Antarctic Peninsula during three summer periods (2008–2010). **Deep Research Part II Top Study on Oceanogragphy,** v. 149, p. 84–98, 2018.

JEAN-BAPTISTE, P.; FOURRÉ, E.; POISSON. A. Gas transfer velocities for 3he in a lake at high wind speeds. In: DONELAN, M. A. et al. (Ed.). **Gas transfer at water surfaces**. [S.l.]: AGU, 2002. p. 233–238.

JIANG, C. et al. Drake passage oceanic pco2: evaluating cmip5 coupled carbon–climate models using in situ observations. **Journal of Climate**, v. 27, n. 1, p. 76-100, 2014.

KARA, A. B.; ROCHFORD, P. A.; HURLBURT, H. E. Efficient and accurate bulk parameterizations of air- sea fluxes for use in general circulation models. **Journal of Atmospheric and Oceanic Technology**, v. 17, n. 10, p. 1421–1438, 2020.

KERR, R. et al. The western South Atlantic Ocean in a high-co2 world: current measurement capabilities and perspectives. **Environmental Management,** v. 57, p. 740–752, 2016.

KEPPLER], L.; LANDSCHÜTZER, P. egional wind variability modulates the Southern Ocean carbon sink. **Scientific Report,** v. 9, n. 1, p. 1-10, 2019.

LENCINA-AVILA, J. M. et al. Past and future evolution of the marine carbonate system in a coastal zone of the Northern Antarctic Peninsula. **Deep Research Part II Top Study on Oceanography**, v. 149, p.193–205, 2018.

LE QUÉRÉ, C. et al. Impact of climate change and variability on the global oceanic sink of CO2. **Global Biogeochemical Cycles,** v. 24, GB4007, 2010.

LE QUÉRÉ, C. et al. Global carbon budget 2016. **Earth System Science Data**, v. 8, p. 605–649, 2016.

LE QUÉRÉ, C. et al. The global carbon budget 2017. **Earth Systems Sciences Data Discussions**, p. 405–448, 2017.

LE QUÉRÉ, C. et al. Global carbon budget 2018. **Earth System Science Data**, v. 10, p. 2141–2194, 2018.

LEUNG, S. CABRÉ, A.; MARINOV, I. A latitudinally banded phytoplankton response to 21st century climate change in the Southern Ocean across the CMIP5 model suite. **Biogeosciences**, v. 12, p. 5715-5734, 2015.

LISS, P. S.; MERLIVAT, L. Air-sea gas exchange rates: introduction and synthesis. In: PATRICK B. M. (Ed.). **The role of air-sea exchange in geochemical cycling**. Berlin: Springer, 1986. p. 113–127.

LOPEZ, O. et al. Hydrographic and hydrodynamic characteristics a of the eastern basin of the Bransfiled Strait. **Deep Sea Research Part I Oceanography Research**, v. 46, p. 1755–1778, 1999.

LOHRENZ, S. E. et al. Satellite estimation of coastal pCO2 and air-sea flux of carbon dioxide in the northern Gulf of Mexico. **Remote Sensing of Environment**, v. 207, p. 71-83, 2018.

LOVENDUSKI, N. S. et al. Enhanced CO2 outgassing in the Southern Ocean from a positive phase of the Southern annular mode. **Global Biogeochemical Cycles**, v. 21, GB2026, 2007.

LOVENDUSKI, N. S. et al. Multi-decadal trends in the advection and mixing of natural carbon in the Southern Ocean. **Geophysical Research Letters**, v. 40, p.139–142, 2013.

LOVENDUSKI, N. S.; LONG, M. C.; LINDSAY, K. Natural variability in the surface ocean carbonate ion concentration. **Biogeosciences**, v. 12, n. 21, p. 6321–6335, 2015.

LANDSCHÜTZER, P. et al. Recent variability of the global ocean carbon sink. **Global Biogeochemical Cycles**, v. 28, n. 9, p. 927–949, 2014.

MAJKUT, J. D.; SARMIENTO, J. L.; RODGERS, K. B. A growing oceanic carbon uptake: Results from an inversion study of surface *p*CO2 data. **Global Biogeochemical Cycles,** v. 28, p. 335–351, 2014.

MCGILLIS, W. R. et al. Carbon dioxide flux techniques performed during GasEx-98. **Marine Chemistry**, v. 75, n. 4, p. 267–280, 2001.

METZL, N. Decadal increase of oceanic carbon dioxide in the Southern Indian Ocean surface waters (1991–2007). **Deep-Sea Research II**, v. 56, p. 607-619, 2009.

MILLER, S. D. et al. Platform motion effects on measurements of turbulence and air-sea exchange over the open ocean. **Journal of the Atmospherical Ocean Technology**, v. 25, n. 9, p. 1683–1694, 2008.

MONIN, A.; OBUKHOV, A. Basic laws of turbulent mixing in the atmospheric surface layer. **Proceedings of Geophysics Institute**, v. 24, p. 163-187, 1954.

MONTEIRO, T.; KERR, R.; MACHADO, C. Seasonal variability of net sea - air CO2 fluxes in a coastal region of the Northern Antarctic Peninsula. **Scientific Report,** e 0123456789, 2020.

MUNRO, D. R. et al. Estimates of net community production in the Southern Ocean determined from time series observations (2002–2011) of nutrients, dissolved inorganic carbon, and surface ocean *p*CO2 in Drake Passage. **Deep-Sea Research II**, v. 114, p. 49-63, 2015.

NATIONAL OCEANIC AND ATMOSPHERIC ADMINISTRATION (NOAA). **Climate at a glance: global time series**. 2019. Available from: https://www.ncdc.noaa.gov/cag/.

NEUKERMANS. R. et al. Harnessing remote sensing to address critical science questions on ocean-atmosphere interactions. **Elements in Science Anthropology**, v. 6, 2018.

NIGHTINGALE, P. D. et al. In situ evaluation of air-sea gas exchange parameterizations using novel conservative and volatile tracers. **Global Biogeochemical Cycles**, v.14, n. 1, p. 373–387, 2000.

OGUNDARE, M. O. et al. Variability of sea-air carbon dioxide flux in autumn across the weddell gyre and offshore dronning maud land in the southern ocean. **Frontiers in Marine Science**, v.7, e 1168, 2021.

OLIVEIRA, R. R. et al. First measurements of the ocean-atmosphere CO2 fluxes at the Cabo Frio upwelling system region, Southwestern Atlantic Ocean. **Continental Shelf Research**, v. 181, p. 135–142, 2019.

ORSELLI, I. B. M. et al. How fast is the Patagonian shelf-break acidifying? **Journal of Marine System**, v. 178, p. 1–14, 2017.

ORSI, H. A.; WHITWORTH, T.; WORTH, D. N. On the meridional extent and fronts of the Antarctic Circumpolar Current. **Deep Research I**, v. 42, n. 5, p. 641–673, 1995.

PADIN, X.A. et al. Air- sea CO2 fluxes in the atlantic as measured during boreal spring and autumn. **Biogeosciences**, v. 7, p. 1587–1606, 2010.

PARDO, P. C. et al. Anthropogenic CO2 estimates in the Southern Ocean: Storage partitioning in the different water masses. **Progress in Oceanography**, v. 120, p. 230–242, 2014.

PATTEY, E. et al. Measuring nighttime CO2 flux over terrestrial ecosystems using eddy covariance and nocturnal boundary layer methods. **Agriculture Forest Meteorololgy,** v. 113, n. 1/4, p. 145–158, 2002.

PFEIL, B. et al. **Surface Ocean CO2 Atlas (SOCAT)**. 2013. Available from: http://cdiac.ornl.gov/ftp/oceans/SOCATv1.5/.

PENG, G. et al. A long-term and reproducible passive microwave sea ice concentration data record for climate studies and monitoring. **Earth System Science Data**, v. 5, p. 311-318, 2013.

PEZZI, L. P. et al. Multiyear measurements of the oceanic and atmospheric boundary layers at the Brazil-Malvinas confluence region. **Journal of Geophysical Research Atmosphere**, v. 114, n. 19, p. 1–19, 2009.

PEZZI, L. P. et al. Oceanic eddy-induced modifications on the air-sea heat and CO2 fluxes in the Brazil-Malvinas Confluence. **Scientific Report**, p. 1–27, 2021.

PEZZI, L. P. et al. Ocean-atmosphere in situ observations at the Brazil-Malvinas Confluence region. **Geophysical Research Letters**, v. 32, n. 22, p. 1–4, 2005.

PEZZI, L. P. et al. Air-sea interaction at the Southern Brazilian Continental Shelf: In situ observations. **Journal of Geophysical Research Ocean**, v. 121, n. 9, p. 6671–6695, 2016.

PEZZI, L. P.; SOUZA, R. B.; QUADRO, M. F. L. Uma revisão dos processos de interação oceano-atmosfera em regiões de intenso gradiente termal do Oceano Atlântico Sul baseada em dados observacionais. **Revista Brasileira de Meteorologia,** v. 31, n. 4, p. 428–453, 2015.

PHILLIPS, O. M. **The dynamics of the upper ocean**. Cambridge: Cambridge University, 1977. 336 p.

PIERROT, D. et al. Recommendations for autonomous underway pCO2 measuring systems and data-reduction routines. **Deep-Sea Research Part II: Topical Studies in Oceanography**, v. 56, n. 8–10, p. 512–522, 2009.

REBOITA, M. S. et al. Regimes de precipitação na América do Sul. **Revista Brasileira de Meteorologia**, v. 25, n. 2, p. 185–204, 2010.

RINTOUL, S.; HUGHES, C.; OLBERS D. **The antarctic circumpolar current system**. [S.l.: s.n.], 2001.

RODEN, N. P. et al. Carbon cycling dynamics in the seasonal sea-ice zone of East Antarctica. **Journal of Geophysical Research Oceans**, v. 121, p. 8749–8769, 2016.

SABINE, C. L. et al. The oceanic sink for anthropogenic CO2. **Science**, v. 305, n. 5682, p. 367–371, 2004.

SANTINI, M. F. **Determinação dos fluxos turbulentos de calor e momentum entre o oceano e atmosfera na região sudoeste do Oceano Atlântico**. Tese

(Doutorado em Meteorologia) - Universidade Federal de Santa Maria, Santa Maria, 2017.

SANTINI, M. F. et al. Observations of air – sea heat fluxes in the southwestern Atlantic under high-frequency ocean and atmospheric perturbations. **Quarterly Journal of the Royal Meteorological Society**, v. 146, p. 4226–4251, 2020.

SATO. O. T. Fluxos de calor oceânico medido por meio de satélites. In: SOUZA, R. B. (Ed.). **Oceanografia por satélites**. São Paulo: Oficina de Textos, 2005. p.148– 165.

SONG, H. et al. Mesoscale modulation of air-sea CO2 flux in Drake Passage. **Journal of Geophysical Research Oceans**, v. 121, p. 6635–6649, 2016.

SOUZA, R. et al. Air-sea interactions over eddies in the brazil-malvinas confluence. **Remote Sensing**, v. 13, n. 7, e1335, 2021.

SUN, Y. et al. Optimizing window length for turbulent heat flux calculations from airborne eddy covariance measurements under near neutral to unstable atmospheric stability conditions. **Remote Sensing**, v. 10, n. 5, 2018.

SHUTLER, J. et al. FluxEngine: a flexible processing system for calculating atmosphere-ocean carbon dioxide gas fluxes and climatologies. **Journal of Atmospheric Oceanic Technolology,** v. 33, n. 4, p. 741-756, 2016.

STEPHENSON, G. R.; GILLE, S. T.; SPRINTALL J. Seasonal variability of upper ocean heat content in Drake Passage. **Journal of Geophysical Research**, v. 117, C04019, 2012.

STULL, R. B. **An introduction to boundary layer meteorology**. Dordrecht: Kluwer Academic, 1988.

SWEENEY, C. et al. Constraining global air-sea gas exchange for CO2 with recent bomb 14C measurements. **Global Biogeochemical Cycles**, v.21, n. 2, GB2015. 2017. Available from: http://onlinelibrary.wiley.com/doi/10.1029/2006GB002784/abstract.

TAKAHASHI, T. et al. Climatological mean and decadal change in surface ocean *p*CO2, and net sea-air CO2 flux over the global oceans. **Deep Research Part II Topical Study in Oceanography**, v. 56, n. 8/10, p. 554–577, 2009.

TAKAHASHI, T. et al. The changing carbon cycle in the Southern Ocean. **Oceanography**, v. 25, n. 3, p. 26–37, 2012.

TAKAHASHI, T.; SUTHERLAND, S.C.; KOZYR, A. **Global ocean surface water partial pressure of CO2 database: measurements performed during 1957–2017 (version 2017)**. 2018. Available from: https://www.nodc.noaa.gov/oceanacidification/stewardship /data_portal.html.

TRENBERTH, K. E.; FASULLO, J. T.; KIEHL J. Earth's global energy budget. **Bulletin of the American Meteorological Society**, v. 90, n. 3, p. 311–323, 2009.

XUE, L, et al. Response of sea surface fugacity of CO2 to the SAM shift south of Tasmania: regional differences. **Geophysical Research Letters**, v.42, p. 3973–3979, 2015.

WALLACE, J. M.; MITCHELL, T. P.; DESER, C. The influence of sea surface temperature on surface wind in the eastern equatorial Pacific: seasonal and interannual variability. **Journal of Climate**, v. 2, p.1492–1499, 1989.

WANNINKHOF, R. Relationship between wind speed and gas exchange over the ocean. **Journal of Geophysical Research**, v. 97, n. C5, p.7373, 1992.

WANNINKHOF, R. (2014). Relationship between wind speed and gas exchange over the ocean revisited: gas exchange and wind speed over the ocean. **Limnology and Oceanography: Methods**, v. 12, n. 6, p. 351-362, 2014.

WANNINKHOF, R. et al. Advances in quantifying air-sea gas exchange and environmental forcing. **Annual Review of Marine Science**, v. 1, n. 1, p. 213-244, 2009.

WANNINKHOF, R.; MC GILLIS, W.R. A cubic relationship between air-sea CO2 exchange and wind speed. **Geophysical Research Letters**, v. 26, n. 13, p. 1889-1892, 1999.

WANNINKHOF, R.; TRIÑANES J. The impact of changing wind speeds on gas transfer and its effect on global air-sea CO2 fluxes. **Global Biogeochemical Cycles**, v. 31, n. 6, p. 961–974, 2017.

WEBB, E. K. On the correction of flux measurements for effects of heat and water vapour transfer. **Boundary-Layer Meteorology,** v. 23, n. 2, p. 251–254, 1982.

WEISS, R. F. Carbon dioxide in water and seawater. **Marine Chemistry**, v. 2, n. 3, p. 203–215, 1974.

WOOLF, D. K. Parameterization of gas transfer velocities and sea-state-dependent wavebreaking. **Tellus**, v. 57, n. B, p. 87–94, 2005.

WOOLF, D. K. et al. Modelling of bubble-mediated gas transfer: fundamentalprinciples and a laboratory test. **Journal of Marine Systems**, v. 66, p. 71–91,2007.

WOOLF, D. K. et al. On the calculation of air-sea fluxes of CO2 in the presence of temperature and salinity gradients. **Journal of Geophysical Research Oceans**, v.121, p.1229–1248, 2016.

YUSUP, Y.; LIU, H. Effects of atmospheric surface layer stability on turbulent fluxes of heat and water vapor across the water-atmosphere interface. **Journal of Hydrometeoroly**, v.17, n.11, p.2835–2851, 2016.

WOOLF, D. K. et al. Modelling of bubble-mediated gas transfer: fundamental principles and a laboratory test. **Journal of Marine Systems**, v.66, p.71–91, 2007.

ZHOU, M.; NIILER, P. P.; HU, J. H. Surface currents in the Bransfield and Gerlache Straits, Antarctica. **Deep Sea Research Part I: Oceanographic Research Papers**, v.49, n.2, p.267–280, 2002.

ZHU, Y. et al. Satellite-derived surface water pCO2and air-sea CO2fluxes in the northern South China Sea in summer. **Progress in Natural Science**, v.19, n.6, p. 775–779, 2009.